
IREX IV: Part 2

Compression Profiles for Iris Image Compression

NIST Interagency Report 7978

G. W. Quinn, P. Grother, M. Ngan

Information Access Division
National Institute of Standards and Technology



January 29, 2014

1 **Acknowledgements**

2 The authors would like to thank the sponsors of this activity. These are the Federal Bureau of Investigation, the U.S. VISIT
3 office in the Department of Homeland Security (DHS), and the Science and Technology Directorate, also in DHS. Vially,
4 the authors would also like to thank the United States Department of Defense's Biometrics Identity Management Agency for
5 their support and active collaboration.

6 **Disclaimer**

7 Specific hardware and software products identified in this report were used in order to perform the evaluations described
8 in this document. In no case does identification of any commercial product, trade name, or vendor, imply recommendation
9 or endorsement by the National Institute of Standards and Technology, nor does it imply that the products and equipment
10 identified are necessarily the best available for the purpose.

11 Executive Summary

12 *Background:* With the publication of ISO/IEC 19794-6:2011 and ANSI/NIST ITL 1-2011 as stable and tested iris image
13 interchange standards, iris can be exploited as a powerful interoperable biometric in a range of one-to-one and one-to-
14 many roles. Some applications require compression of the iris data because resource constraints exist. These are the
15 limited size and communication speed of ISO/IEC 7816 based smartcard credentials, and the limited bandwidth that is
16 sometimes available for transmission of biometric data to backend servers. While one solution to this has been transmission
17 of relatively small biometric templates, this is problematic for iris recognition because there are no *standardized* templates for
18 iris data. The current solution is the transmission of compressed standardized iris image data. Compression can be lossless,
19 but sometimes only lossy compression can fulfil file size requirements. Iris recognition is advantaged by standardized
20 formats that assist compression, and by the fact that the iris texture can sustain considerable compression damage and still
21 remain viable for recognition. The published image interchange standards do not yet contain definitive detailed guidance on
22 compression. This report addresses this need.

23 *Approach:* We seek a formal compression profile for the application of the ISO/IEC 15444-1 JPEG 2000 compression
24 algorithm to iris image data. This establishes settings for the various JPEG 2000 parameters by empirically quantifying their
25 effect on iris recognition accuracy. This is done for applications in which either or both of the enrollment and search samples
26 are compressed. Accuracy is measured using state-of-the-art commercial algorithms applied to over 3 million iris images.

27 *Results:* Most iris cameras emit 8-bit grayscale images with pixel dimensions 640x480. These are standardized as Image
28 Kind 2¹ in ISO/IEC 19794-6:2011. Their size is 307 kilobytes (KB), but they can be compressed to 150KB without any loss
29 of pixel information, and to as little as 16KB with only small losses in accuracy. When the iris is centered and the periphery
30 cropped and masked, as required for Image Kind 7 of the ISO standard, the resulting image can be compressed to as little
31 as 2KB with only small losses in accuracy. Such sizes support inclusion of iris data on secure identity credentials, and fast
32 network-based recognition. Efforts to reduce sizes substantially below 2KB produce elevated error rates that would not be
33 tolerable for many applications.

34 For electronic passports, the International Civil Aviation Organization (ICAO) 9303 specification should be revised to note
35 availability of iris images that are more than 10 times smaller than those conceived of in the first editions of that profile. Par-
36 ticularly, the Data Group 4 container in the Logical Data Structure (LDS) could now be populated with ISO/IEC 19794-6:2011
37 iris images of size 3KB or smaller, rather than the 30KB currently indicated. Facial images stored on e-Passports typically
38 have sizes of 10-20KB, and standardized fingerprint templates have sizes around 0.5KB. Digital signatures associated with
39 any of these elements can readily have sizes around 0.5KB.

40 Technical Summary

41 Further technical results are listed below. Each item roughly corresponds to a section or subsection from the main body of
42 the report.

- 43 • *JPEG 2000 Compression Profile:* The IREX I evaluation identified JPEG 2000 as more effective at compressing iris
44 images than alternatives such as traditional JPEG. This study extends that research by recommending that iris images
45 be compressed with
 - 46 – a single tile,
 - 47 – a block size of 64-by-64,
 - 48 – a base quantization step size of 1/256, and
 - 49 – 3 decomposition levels,

50 when compressing with the irreversible (CDF 9/7) wavelet transform. These parameter values ensure minimal loss in
51 recognition accuracy. The values do not change depending on the file size.

52 The file-size specification follows.

- 53 • *Compression Limits for Kind 2 Formats:* Kind 2 records are produced by most iris cameras and do not undergo special
54 processing to assist with compression. These images can be compressed to 16KB with only small losses in accuracy.

¹ISO/IEC 19794-6:2011 actually refers to these as "Type 2 images" rather than "Kind 2 images", but the terminology is changed in this report to avoid confusion with Type 2 records in ANSI/NIST ITL 1-2011.

55 At a fixed decision threshold, the False Negative Identification Rate (FNIR) increases by no more than a factor of
56 1/4. When compressed to 8KB, FNIR doubles at a fixed decision threshold while the behavior of the False Positive
57 Identification Rate (FPIR) is matching algorithm dependent. Of the four implementations, it does not change for two,
58 increases by about a factor of 5 for one, and increases by about a factor of 20 for the last. Since iris Detection Error
59 Trade-off (DET) curves tend to be low sloping, the increase in FPIR can often be corrected without a significant impact
60 on FNIR by adjusting the decision threshold. When images are compressed to 6KB, the FNIR increases by a factor of
61 3 to 4 (at fixed FPIR), depending on the matching algorithm. Compressing Kind 2 records to sizes smaller than 16KB
62 is not recommended.

63 • *Compression Limits for Kind 7 Formats:* Kind 7 records can be compressed to as little as 2KB with only small losses
64 in accuracy (FNIR at fixed FPIR increases by no more than a factor of 1/4). Note this is an order of magnitude lower
65 than ICAO's recommendation of 30KB as the optimal compression size. Error rates increase more appreciably when
66 images are compressed to sizes smaller than 2KB. When compressed to 1KB, FNIR increases by a factor of 2 to 3 at
67 a fixed threshold, and FPIR does not change for 2 implementations, increases by a factor of 5 for one implementation,
68 and by a factor of about 20 for another. When compressed to 768 bytes, FNIR increases by a factor of 3 to 5 (at
69 fixed FPIR), depending on the implementation used to generate the Kind 7 records. The sclera must be masked and
70 the eyelid boundaries blurred to keep error rates low. Compressing Kind 7 records to sizes smaller than 2KB is not
71 recommended.

72 In comparison to other biometric modalities, standardized fingerprint minutiae information can be stored in 500 bytes,
73 and face images can be compressed to about 8KB, although ISO/IEC 19794-6 recommends 30KB, and ICAO recom-
74 mends 10-20KB for e-passports.

75 • *Relevance to 1:1 Verification:* This study was conducted using 1:N algorithms where the enrolled population was
76 typically 160 000. Given our focus on FPIR values around 10^{-3} , this study has approximate correspondence to 1:1
77 false match rates below 10^{-8} , a security level more stringent than would be used for most high security applications.

78 • *Two-Eye Matching:* When a fixed amount of storage space is available, sometimes greater accuracy can be achieved
79 by storing images of both eyes rather than a more lightly compressed version of just one. This study found that
80 a cross-over occurs for Kind 7 records, where one-eye matching is more accurate than two-eye matching at lower
81 storage capacities, but less accurate at larger storage capacities. At sizes of 1.5KB or less, one-eye matching is
82 consistently more accurate. At 4KB or more, two-eye matching is always more accurate. Note that matching with
83 two eyes introduces an additional computation penalty (to both template generation and searching) that may offset
84 possible accuracy benefits.

85 • *Resolution Downsampling:* Downsampling selectively discards the highest frequency information in the image. If this
86 information is relatively unimportant to the matching algorithm, then ensuring that it is discarded during compression
87 will ensure that a maximum of the encoding budget is dedicated to representing the more important features. Two-
88 by-two pixel averaging as well as selective retention of only the lower-frequency resolution levels of an image's JPEG
89 2000 representation were tested. However, neither method consistently yielded better performance over the case
90 when images are not downsampled. Care should be taken when downsampling images since excessive tuning of the
91 compression process runs the risk of compromising interoperability.

92 • *Lossless Compression:* Lossless compression retains all of the information in an image so that it can be perfectly
93 reconstructed. As such, it cannot achieve compression ratios as high as lossy compression. JPEG 2000 typically
94 manages to compress Kind 7 records losslessly to sizes between 10KB and 40KB, with a mean size of 20KB. Kind
95 2 records typically compress to sizes between 100KB and 170KB, with a mean size of 135KB. Lossy compression
96 should only be applied to images if there is a documented need for small image sizes.

97 The ISO/IEC 19794-5 and ANSI/NIST-ITL 2011-1 standards also allow iris images to be stored as lossless PNGs.
98 The IREX I evaluation compressed iris images with PNG and found that Kind 7 records compress to a median file
99 size of 25KB, and Kind 2 images to a median size of 150KB, which are comparable to the sizes lossless JPEG 2000
100 compression achieves in this evaluation.

101 Contents

102	1 The IREX Program	1
103	2 Introduction	2
104	2.1 Purpose	2
105	2.2 Market Drivers	2
106	2.3 Standard Iris Formats	3
107	3 Methodology	3
108	3.1 Test Environment	3
109	3.2 Iris Dataset	4
110	3.3 Matching Algorithms	4
111	3.4 Compression Algorithm	5
112	3.5 Performance Metrics	5
113	4 Results	8
114	4.1 Toward a JPEG 2000 Compression Profile	8
115	4.1.1 Tile Size	9
116	4.1.2 Quantization Step Size	10
117	4.1.3 Number of Decomposition Levels	11
118	4.1.4 Block Size	12
119	4.1.5 Timing Statistics	13
120	4.1.6 Summary of Recommendations	15
121	4.2 Performance of Kind 7 Format	15
122	4.2.1 Compressing Only Search Images	15
123	4.2.2 Compressing Search and Enrollment Images	18
124	4.2.3 When to use Both Eyes	20
125	4.2.4 Should Images be Downsampled?	21
126	4.3 Performance of Kind 2 Format	23
127	4.3.1 Compressing Only Search Images	23
128	4.3.2 Compressing Search and Enrollment Images	26
129	4.4 Lossless Compression	28
130	5 References	29

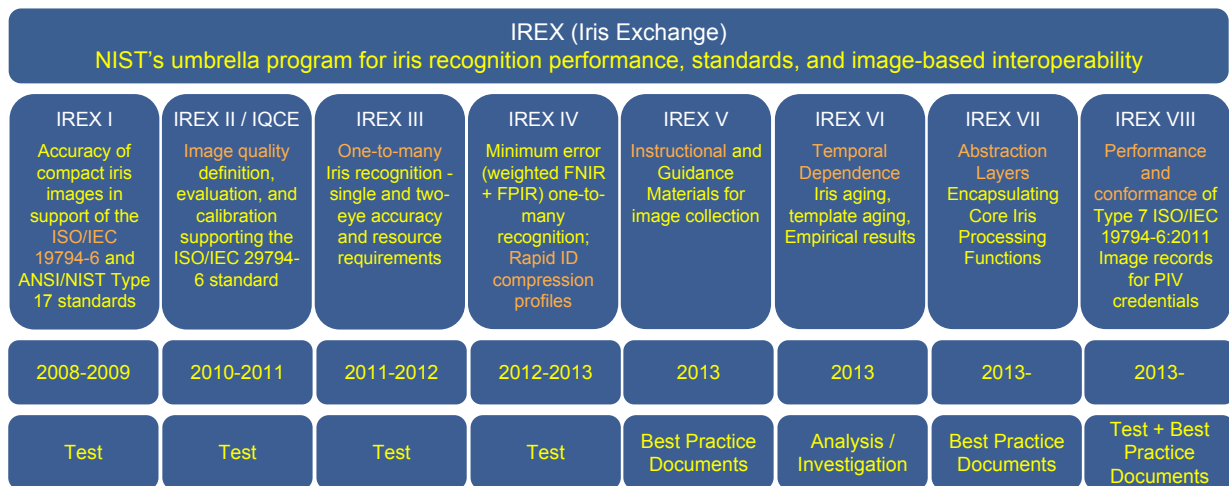


Figure 1: Timeline of the IREX program, including planned future installments.

131 1 The IREX Program

132 The Iris Exchange (IREX) Program was initiated by the National Institute of Standards and Technology (NIST) to support
 133 an expanded marketplace of iris-based applications. IREX provides quantitative support for iris recognition standardization,
 134 development, and deployment. To date, 5 activities have been completed and 3 more are tentatively planned (see Figure 1).
 135 Each is summarized below.

- 136 • **IREX I** [1] was a large-scale, independently administered, evaluation of one-to-many iris recognition. It was conducted
 137 in cooperation with the iris recognition industry to develop and test standard formats for storing iris images. Standard
 138 formats are important for maintaining interoperability and preventing vendor lock-in. The evaluation was conducted in
 139 support of the ISO/IEC 19794-6 and ANSI/NIST-ITL 1-2011 standards.
- 140 • **IREX II** [2] supported industry by establishing a standard set of quality metrics for iris samples. Although iris recognition
 141 has the potential to be extremely accurate, it is highly dependent on the quality of the samples. The evaluation tested
 142 the efficacy of 14 automated quality assessment algorithms in support of the ISO/IEC 29794-6 standard [3].
- 143 • **IREX III** [4] was a performance test of the latest iris recognition algorithms over operational data. Despite growing
 144 interest in iris-based technology, at the time there was a paucity of experimental data to support published theoretical
 145 considerations and accuracy claims. IREX III constituted the first public presentation of large-scale performance
 146 results using operational data.
- 147 • **IREX IV** builds upon IREX III as a performance test of one-to-many iris recognition. In addition to providing partici-
 148 pants from previous evaluations an opportunity to further develop and test their recognition algorithms, this evaluation
 149 explores the potential for using a cost equation model for optimizing algorithms for specific applications.
- 150 • **IREX V** will provide best practice recommendations and guidelines for the proper collection and handling of iris images.
- 151 • **IREX VI** [5] explores a possible aging effect for iris recognition. The intrinsic features of the iris may naturally change
 152 over time in a way that affects recognition accuracy. Factors such as subject habituation and aging of the camera may
 153 also introduce a time dependency.
- 154 • **IREX VII** intends to define a framework for communication and interaction between components in an iris recognition
 155 system. By introducing layers of abstraction that isolate underlying vendor-specific implementation details, a system
 156 can become more flexible, extensible, and modifiable.
- 157 • **IREX VIII** will test the performance of ISO/IEC 19794-6:2011 Type 7 images and lay the groundwork for conformance
 158 testing of Type 7 record generators.

159 The latest information on the IREX Program can be found on the IREX website [6].

160 2 Introduction

161 2.1 Purpose

162 The IREX I evaluation determined JPEG 2000 is the best format for lossy compression of iris images in terms of minimizing
 163 the loss in recognition accuracy. However, JPEG 2000 contains many customizable parameters that were not explored in
 164 the evaluation. These parameters affect not only the pixel representation of an image, but also computation time, memory
 165 usage, and the ability to perform computations in parallel. This study extends IREX I by identifying an optimal combination
 166 of parameter values for compressing standard iris images with JPEG 2000.

167 Secondly, this report tests the ability of automated iris recognition algorithms to match highly compressed iris images.
 168 Unlike IREX I, the current study deals with the more difficult problem of matching in a one-to-many, rather than one-to-one,
 169 mode.

170 2.2 Market Drivers

171 Many biometric systems operate with restrictions on the size of their biometric samples. A system that reads samples from
 172 a smartcard is limited by the storage capacity of its digital chip. For comparison, the NIST Special Publication 800-73-4 [7]
 173 limits the container size on government Personal Identity Verification smartcards to no less than 12 710 bytes for a face
 174 image, and no less than 4 006 bytes for fingerprint minutiae information. FIPS 201-2 [8] recommends no less than 3 000
 175 bytes for an iris image. The Registered Traveler Pilot Program [9], which operated from 2005 to 2009, allocated 4 000 bytes
 176 per iris image. The images were stored in a variation of the polar format later rejected for inclusion in ISO/IEC 19794-6.
 177 ICAO Doc 9303 [10] conservatively recommends 30 720 bytes for optimal storage of an iris image on e-passports even
 178 though subsequent studies have found that iris images can be stored at much smaller sizes without detrimentally affecting
 179 recognition accuracy. Even without a fixed upper limit on the container size, smaller samples transfer more quickly from the
 180 card to the reader. This can influence how many samples are selected for transfer (e.g. one iris or both), or which modality
 181 (e.g. face or fingerprint) is used for recognition.

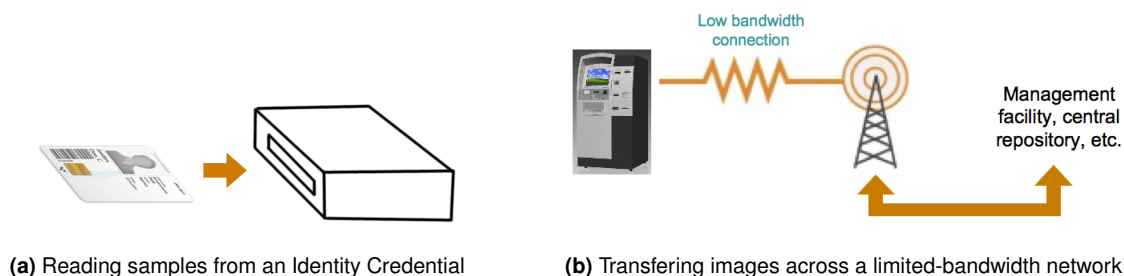


Figure 2: Scenarios where the size of biometric samples impacts performance. Figure 2a depicts a system that reads biometric samples from a limited storage capacity smartcard. Figure 2b depicts a system that transfers samples across a bandwidth-limited network.

182 The size of biometric samples also affects the performance of systems that must transfer samples across bandwidth-limited
 183 networks (see Figure 2b). A prominent example is India's Unique Identity (UID) scheme. Private banks linked to the scheme
 184 will soon deploy thousands of "micro ATMs" across rural parts of the country to provide citizens with better access to their
 185 accounts [11]. These Micro ATMs will verify users' identities by capturing biometric samples locally and transferring them to
 186 a central facility for matching. The samples must be transferred using India's existing telecommunications infrastructure, but
 187 since coverage is weak in some parts of the country, the rate at which data can be transferred is sometimes severely limited.
 188 The iris would be viable only if the samples could be compressed to a few kilobytes.

189 The Department of Defense uses the iris for rapid identification in the field, and smaller samples facilitate faster response
 190 times. Some applications might benefit from transferring a highly compressed version of the iris sample for quick identifica-
 191 tion, followed by a better quality (non-compressed) version of the sample for retention as the authoritative sample.

2.3 Standard Iris Formats

Standard iris images are not iris templates. Rather, they are interoperable images designed for efficient storage and transmission. Templates are proprietary "black box" feature representations specific to a single provider's recognition algorithm. As such, their content is non-standard, non-interoperable, and not suitable for cross-agency or cross-vendor exchange of iris data. Although proprietary templates are sometimes smaller than raw iris images, discarding the original images locks the system into using a particular version of a provider's software. Not only does this undermine interoperability, but it prevents the system from exploiting future improvements in the feature extraction and matching procedures.

The ISO/IEC 19794-6:2011 [12] and ANSI/NIST-ITL 1-2011 [13] standards define Kind 2 and Kind 7 record formats for storing iris images. Kind 2 image records are usually output directly by iris cameras and do not undergo processing to facilitate compression. In contrast, Kind 7 image records provide a much more compact representation of the iris but require further processing to generate. In addition to cropping out much of the periocular region around the iris, the sclera and eyelids must each be masked with a solid color. Uniform regions of solid color require very little space to encode, thus ensuring that a maximum of the encoding budget is dedicated to representing the actual iris features. The first amendment to ISO/IEC 19794-6:2011 defines 4 cases for masking eyelids. The first is depicted in Figure 3a, and 3 alternatives are depicted in Figure 3b. When the upper or lower eyelids do not intersect the iris boundary, they do not need to be localized and masked with a color distinct from that of the sclera. This study focuses its attention solely on the Kind 2 and Kind 7 formats.

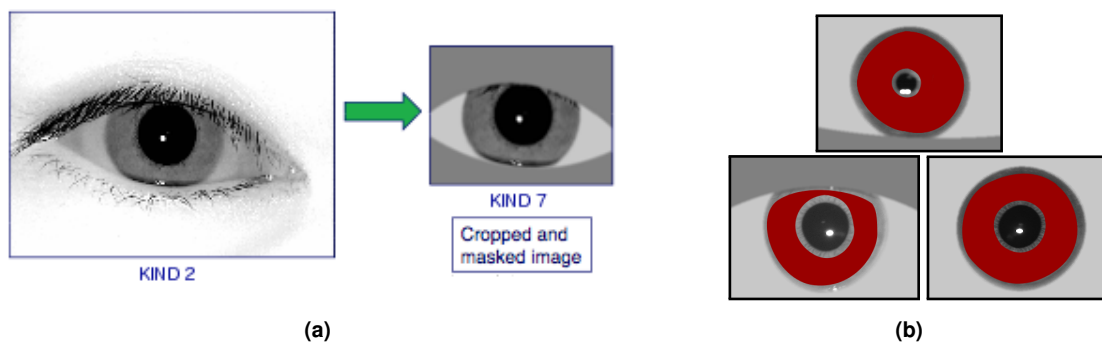


Figure 3: Examples of (a) Kind 2 and Kind 7 image records defined in ISO/IEC 19794-6, and (b) alternative eyelid masking procedures supported by the standard. (Some iris textures are masked with red to prevent identification of the individuals).

3 Methodology

This section describes the test procedures, software, and performance metrics used in this study. Much of this information is covered in greater depth in the *IREX IV Concept of Operations (CONOPS)* [14] document. The reader is referred to this document for further details on the evaluation process.

A technology evaluation [15] such as this focuses on algorithm performance over factors that may be relevant to the deployment and operation of a biometric system (e.g. policy drivers, societal and economic considerations, availability of legacy data). Performance is assessed using metrics that give a general idea of the technology's capabilities. The relative importance of these metrics will depend on how the technology will be used.

3.1 Test Environment

The evaluation was conducted offline at a NIST facility. Testing was performed on high-end PC-class blades running the LINUX operating system, which is typical of central server applications. Most of the blades had 6 quad-core AMD Opteron processors running at 2.4 GHz with 192 GB of main memory. The test harness used concurrent processing to distribute workload across dozens of blades.

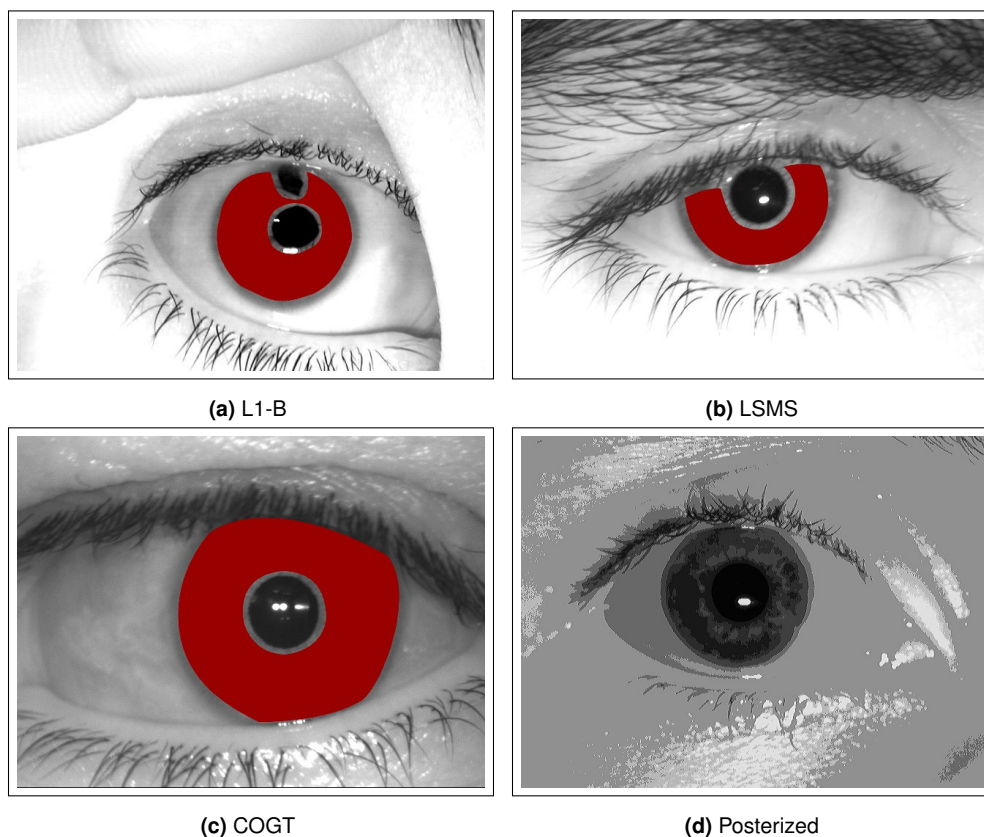


Figure 4: Examples of iris images from the test dataset. The subfigure captions for (a) through (c) refer to a four-letter software code that is an indicator of the type of camera used. The subfigure in (d) is an example of a highly posterized image.

222 3.2 Iris Dataset

223 The evaluation uses images from the Operational Set (OPS) II, which consists of approximately 7.5 million field-collected
 224 images from several commercial capture systems, predominantly the Securimetrics HIIDE and PIER, and the Crossmatch
 225 I SCAN and SEEK. The images occasionally suffer from poor sample quality (e.g. high amounts of occlusion, specular
 226 reflections) that are typical of an operational system. Many were captured outside and contain heavily constricted pupils.
 227 Figure 4 shows some examples from the set. The iris in 4a an anatomical defect that occurs rarely in the dataset (see
 228 the *IREX III Supplemental Report* [16]). All images have a pixel resolution of 640x480. The pathological 330x330 images
 229 discussed in IREX III and its supplement are excluded from this evaluation. Some of the subjects' irides were captured by
 230 more than one camera model on different days. Further details on the images can be found in the IREX III supplement.

231 Some images in the OPS-II dataset suffer from what appears to be a *posterization* effect, an artifact of color quantization
 232 that can lead to significant reductions in the amount of useful feature information in the images. Figure 4d shows an example
 233 of a highly posterized iris image. The IREX III supplement identifies posterization as one of the more common causes of
 234 failed identifications for the current dataset. The dithered texture introduced by posterization also introduces a lot of high
 235 frequency information that makes it more difficult to efficiently compress these images to small file sizes.

236 3.3 Matching Algorithms

237 Twelve commercial organizations and academic institutions submitted 66 iris recognition software libraries for evaluation.
 238 The participation window opened on May 16th, 2012 and closed on August 2nd, 2012. Participation was open worldwide
 239 to anyone with the ability to implement a large-scale one-to-many iris identification algorithm. There was no charge to
 240 participate.

241 Support for Kind 7 record generation was optional but encouraged. Five of the 12 participants provided software libraries

Participant	Letter Code	Class P Submissions	Kind 7 Support?
University of Bath	A	A00P, A01P, A02P	
Neurotechnology	B	B00,P B01P, B02P	✓
Smart Sensors	C	C00P, C01P, C02P	
3M Cogent	D	D00P, D01P, D02P	
IriTech	E	E00P, E01P, E02P	
MorphoTrust	F	F00P, F01P, F02P	✓
iSciLab	G	G00P, G01P, G02P	
Delta ID	H	H00P, H01P	
University of Cambridge	I	I00P, I01P, I02P	✓
Iris ID	J	J00P, J01P	
Morpho	K	K00P, K01P, K02P	✓
Nihon Systems	L	L00P	

Table 1: Participants of IREX IV along with their NIST-assigned letter codes, algorithm identifiers, and whether the submissions support Kind 7 record generation.

242 capable of generating Kind 7 records from raw Kind 2 images, although one provider's implementations were untestable
 243 because they produced runtime errors. All submissions were required to support the proper handling of Kind 7 records even
 244 if they could not generate the records themselves. However, this report focuses predominantly on the most recent algorithm
 245 submissions from the 4 participants who support Kind 7 record generation.

246 Table 1 lists the IREX IV participants along with the alpha-numeric codes assigned to their algorithms. Participants were
 247 allowed to submit up to 3 Class P algorithms. Briefly, Class P means the algorithms are intended for use in positive (as
 248 opposed to negative) identification systems. Positive identification systems verify the claim that the user is enrolled and
 249 typically grant special privileges or access to enrolled users. Four of the participants (University of Bath, iSciLab, Delta ID
 250 and Nihon Systems) are new to the IREX program while the other 8 have participated in previous IREX evaluations. For
 251 each participant, the algorithms are labeled by chronological order of submission.

252 Four participants (lettered B, F, I, and K) provided implementations that support for the generation of Kind 7 records. However,
 253 the implementations from participants and B and K are only partially conformant to the standard since they do not always
 254 mask the sclera or blur the sclera-eyelid boundaries.

255 3.4 Compression Algorithm

256 This evaluation uses version 7.0 of Kakadu Software's JPEG 2000 developer toolkit [17]. The software is proprietary and
 257 fully compliant with Part 1 of the JPEG 2000 standard [18]. Open-source alternatives to Kakadu include OpenJPEG [19],
 258 and JasPer [20]. Only part 1 of the JPEG 2000 standard is used to compress images in this evaluation. The more flexible
 259 second part of the standard is not widely supported as of this writing and is not tested.

260 The quality and fidelity of the compressed images are the most important performance characteristics, although compression
 261 time is also sometimes measured and reported.

262 3.5 Performance Metrics

263 3.5.1 Operational Scope

264 This evaluation measures iris recognition performance for *open-set* applications, meaning individuals are searched against
 265 a database of previously enrolled persons, but without any guarantee that searched individuals are enrolled. Most real-
 266 world applications of biometrics operate in this way. For example, a system that grants building access cannot assume
 267 that every user who attempts access has provided the system with an enrollment sample on a previous occasion. *Closed-*
 268 *set* applications, which assume every searched individual is enrolled (and thus only concern themselves with identifying

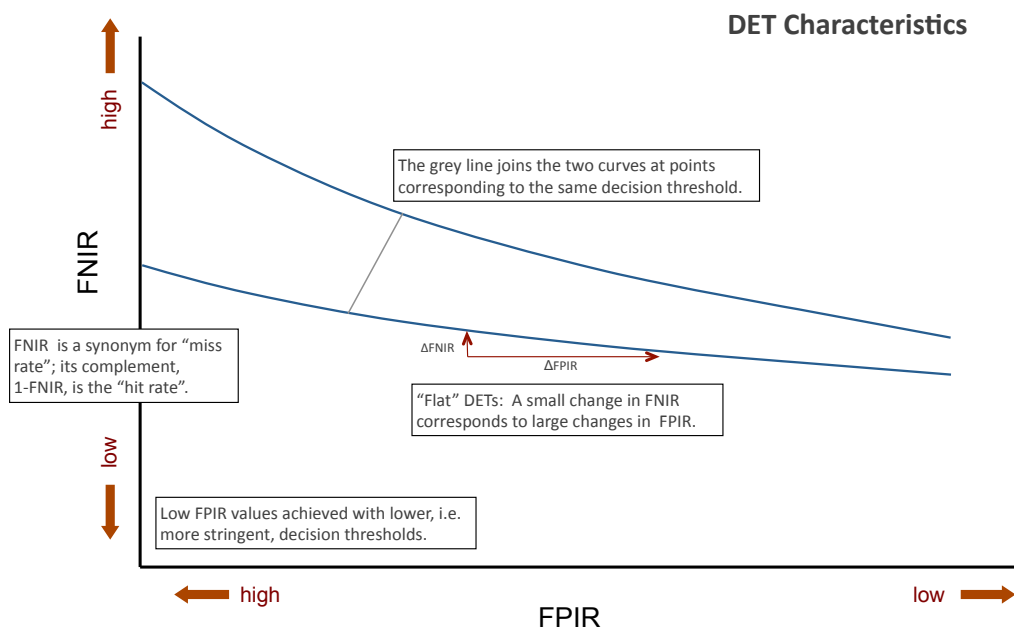


Figure 5: Notional DET curves. Each point along the curve corresponds to a particular decision threshold. Adjusting the decision threshold decreases the rate of one error type, but at the expense of the other.

269 the searched person from among the enrolled population) are operationally uncommon for iris and are not tested in this
 270 evaluation.

271 Consideration is further restricted to *positive* identification systems only, which verify the (often implicit) claim that the user
 272 is enrolled in the database. Such systems typically grant special privileges or access to enrolled users. For example, the
 273 NEXUS Program [21] uses iris recognition to positively identify registered travelers for expedited security screening at ports
 274 of entry in the US and Canada. Negative identification systems, which were not specifically tested in this evaluation, verify
 275 the claim that the person is *not* enrolled and often impose restrictions on enrolled individuals. An example is the United Arab
 276 Emirates (UAE)'s border-crossing control system, which uses iris recognition to prevent expelled individuals from re-entering
 277 the country.

278 3.5.2 Matching Accuracy

279 Matching accuracy is measured for open-set biometric systems, which are tasked with searching an individual against an
 280 enrollment database and returning zero or more candidates. A candidate is returned if the implementation determines that
 281 dissimilarity to the searched image is below a pre-determined decision threshold. A false positive occurs when a search
 282 returns a candidate for an individual that *is not* enrolled in the database. A false negative occurs when a search *does not*
 283 return the correct candidate for an individual that *is* enrolled in the database. Raising the decision threshold increases the
 284 rate of false positives but decreases the rate of false negatives.

285 Core matching accuracy is presented in the form of Detection Error Tradeoff (DET) plots [22], which show the trade-off
 286 between the False Positive Identification Rate (FPIR) and the False Negative Identification Rate (FNIR) as the decision
 287 threshold is adjusted. Figure 5 shows a notional DET plot. Low security applications (e.g. theme park access) might operate
 288 at high decision thresholds, toward the right end of the figure. High security applications (e.g. access to highly sensitive
 289 information) are more likely to operate at low decision thresholds, toward the left end of the figure. Iris recognition is known
 290 for having lightly sloping DETs compared to other biometric modalities.

291 The integrity of ground truth information is a matter of concern in any biometric evaluation. Identity mistakes are known to
 292 exist in OPS II. To negate their impact on the FPIR, we chose to horizontally flip search images prior to template generation
 293 when the searches were non-mated. Replacing a search image with its mirror image ensures that even if a mate is enrolled,
 294 the textures will still appear different (see IREX III Section 6.3 for a detailed explanation and analysis). Unfortunately, this
 295 does not solve the problem where two or more different people are assigned the same identifier. Although this type of error
 296 can inflate estimates of FNIR, the IREX III Supplemental Report found it to be a rare occurrence (of 17,017 mated searches,

297 only 28 failures were attributed to this type of ground truth error).

298 Due to the high frequency of erroneous (left/right) eye labelings in the OPS-II dataset, we chose to always enroll both eyes
299 for an individual as separate entries and credit the algorithm with a match if either of the subject's eyes were matched.
300 We suspect the mislabelings are due to ambiguity with respect to whether "left" is intended to refer to the subject's left eye
301 (correct) or the eye on the left from the perspective of the camera operator (incorrect).

302 False positives are computed exclusively from non-mated searches (i.e. searches for which the searched individual is not
303 enrolled in the database). This is more reflective of operation than if false positives had been computed from mated searches
304 with the correct candidates removed from the list. Similarly, false negatives are computed exclusively from mated searches.

305 3.5.3 Computation Time

306 Timing statistics are presented for compression operations as the actual time elapsed according to the Bash shell's `time`
307 command, which has a resolution of one millisecond on our platform. The command reports end-to-end runtime, which
308 includes the time it takes to read an image from disk. To reduce the impact of I/O on timing statistics, the images are read
309 from `/dev/shm` to ensure they are already cached in main memory. The alternative C function `clock()`, which measures the
310 amount of processor time dedicated to the process, has insufficient resolution and would not report useful timing statistics
311 for multithreaded runs.

312 Timing statistics were collected on an unloaded machine having the specifications described in Section 3.1 (a high-end
313 PC-class blade with 6 quad-core AMD Operteron CPUs running at 2.4 GHz).

314 3.5.4 Uncertainty Estimation

315 Some figures and tables convey information about the uncertainty associated with a statistic in the form of confidence
316 intervals or estimates of standard deviation. These estimates are intended to capture random variation in the observed
317 value if one assumes repeated *iid* sampling from the same population. They are *not* intended to reflect how the statistic
318 might change over different test data or even different sampling strategies over the same data.

319 Estimates of uncertainty are computed using the Wilson Score method [23] which overcomes certain problems associated
320 with applying the Central Limit Theorem to a discretized estimator. We make several simplifying assumptions when applying
321 the method to biometric identification. Most notably, separate searches against the same enrollment database are treated
322 as independent samples, yet we know positive correlations exist due to Doddington's Zoo [24]. We also report estimates of
323 the variability of FNIR at a fixed FPIR when in fact it is the decision threshold that is fixed. Uncertainty with respect to what
324 decision threshold corresponds to the targeted FPIR results in increased uncertainty about the true value of FNIR. However,
325 our estimates of FPIR are fairly tight due to the large number of non-mated searches performed, so they are not expected
326 to have a large impact on the estimates.

327 4 Results

328 4.1 Toward a JPEG 2000 Compression Profile

329 JPEG 2000 includes a number of customizable parameters that affect the pixel representation of an image when it is com-
 330 pressed. The goal of this section is to identify the optimal combination of parameter values that minimize the loss in
 331 recognition accuracy. The effect that some of these parameters have on other performance metrics, such as computation
 332 time, is also investigated.

333 Lossy compression was always performed with the irreversible (9/7) wavelet transform. Section 4.4 explores lossless com-
 334 pression and uses the reversible (5/3) wavelet transform.

335 Overview of the Encoding Procedure

336 The basic steps of the compression process are depicted in Figure 6. The diagram is high-level and over-simplified in some
 337 places to only depict the steps most pertinent to the current study. After the image is divided into non-overlapping rectangular
 338 tiles, each tile is wavelet transformed. The coefficients are then quantized to reduce the number of bits required to represent
 339 them. The image data is then partitioned into code blocks that are passed directly to the entropy coder, which uses the
 340 Embedded Block Coding with Optimal Truncation (EBCOT) algorithm to perform the core optimization of JPEG 2000. The
 341 final result is a serialized bit-stream.

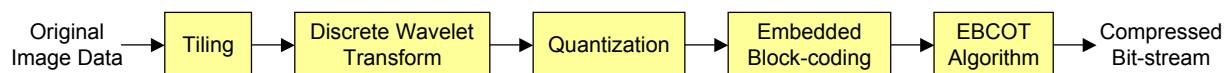


Figure 6: Basic steps of JPEG 2000 compression.

342 The bit-rate is the most important parameter because it is used to target a desired file size. The other parameters varied in
 343 this study are listed below.

- 344 • **Tile Size:** Before wavelet conversion, the image is separated into non-overlapping rectangular tiles that are each en-
 345 coded separately. Setting the tile size to a small value can introduce blocking artifacts similar to traditional JPEG, since
 346 no attempt is made to smooth the borders between adjoining blocks. Partitioning in this manner allows operations to
 347 be performed on individual tiles without having to load the entire image into memory.
- 348 • **Number of Decomposition Levels:** After the wavelet transformation, tiles are broken into multiple decomposition
 349 levels such that higher levels describe finer details in the image. The process, known as Dyadic decomposition [25],
 350 is a "divide and conquer" strategy that has desirable mathematical properties.
- 351 • **Quantization Step Size:** The quantization step size determines the granularity of the wavelet coefficients. Quanti-
 352 zation performs both rounding and truncation of the coefficients. Small step sizes correspond to finer granularity (i.e.
 353 greater precision and fidelity to the original image), but require more bits to represent. Quantization is performed prior
 354 to entropy coding.
- 355 • **Block Size:** Specifies the dimensions of the rectangular code blocks. After the wavelet transformation, the image is
 356 separated into frequency subbands. Each frequency subband is further separated into code blocks, and each block is
 357 independently coded as a bit stream. The entropy coder operates directly on these blocks, truncating each at a point
 358 that minimizes the overall squared error loss. The code block size is normally set to either 32-by-32 or 64-by-64.

359 **4.1.1 Tile Size**

360 **Introduction**

361 Before wavelet conversion, the image is divided into non-overlapping rectangular tiles. Tiling is intended to reduce
 362 memory usage when viewing or modifying high-resolution images since many operations only require some tiles to
 363 be loaded into memory. The downside to tiling is that it can introduce blocking artifacts along the borders between
 364 tiles (see Figure 7). Iris images have relatively small pixel dimensions and are not expected to benefit from using
 365 more than a single tile to cover the entire image. Generally speaking, tiling is intended for use with much higher
 366 resolution images, such as those produced by medical imaging devices [26]. Tile dimensions are usually powers of
 367 2 and cannot vary within an image (with the exception of those running along the right and bottom image border
 368 that are sometimes truncated). Kakadu's default tile size is the smallest possible that encompasses the entire image.
 369

370 **Results and Recommendations**

371 Figure 8 shows recognition accuracy as a function of file size when search images are compressed with different tile sizes. All other compression parameters are left
 372 at their default values (i.e. 3 decomposition levels, a quantization step size of 1/256, and a block size of 64). Although the tile size has little effect at large file sizes, the
 373 benefit to using a single tile is apparent at sizes below 2 048. When compressing to a
 374 size of 1 024 bytes, a tile size of 128 increases FNIR by between 10 and 60 percent,
 375 depending on the matching algorithm. This report recommends that only a single
 376 tile be used to represent the image. For Kind 2 and Kind 7 images, a tile size of
 377 1024x1024 pixels is sufficient. Setting the tile size to be greater than the dimensions
 378 of the image does not detrimentally affect compression.
 380

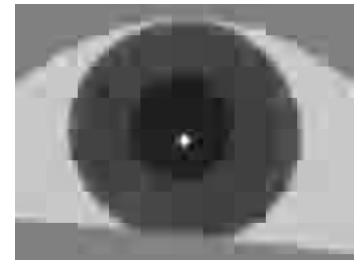


Figure 7: Demonstration of blocking artifacts in a highly compressed JP2 image.

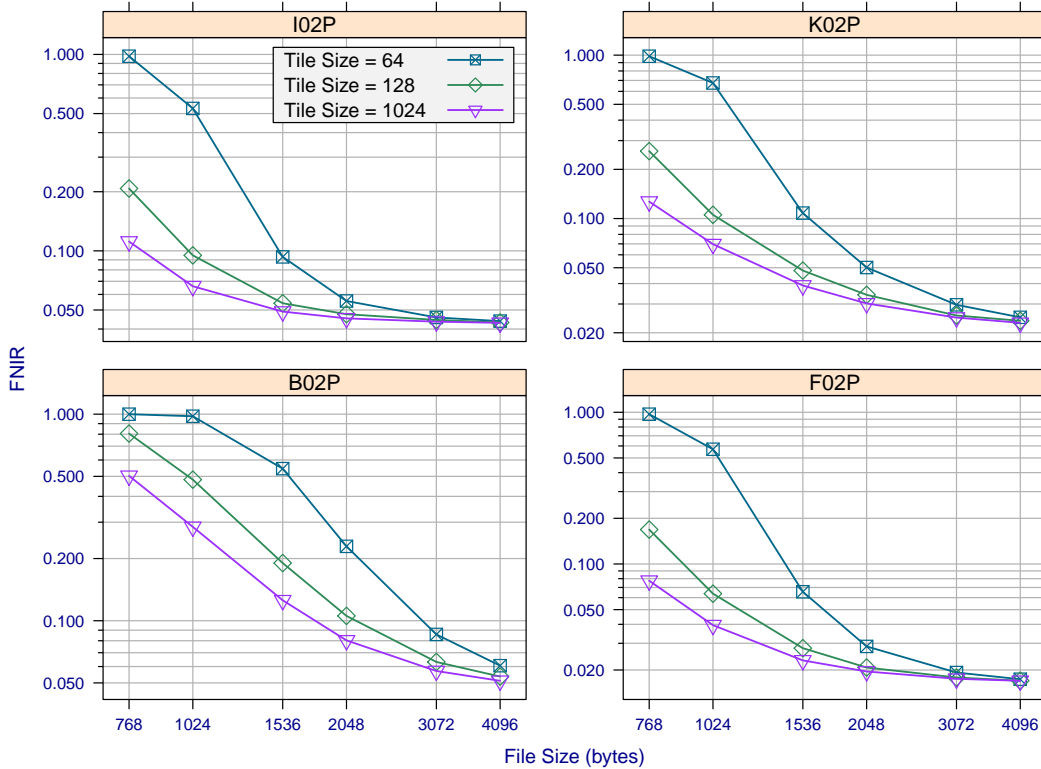


Figure 8: Comparison of FNIR (at FPIR=0.001) for 4 matching algorithm when search images are compressed with various tile sizes. Compressed Kind 7 records (created by the matching algorithms) are searched against an enrolled population of 160 000 non-compressed images. Each point is generated from 80 135 mated searches.

Kind 2 = Unprocessed from iris camera **FNIR** = False Negative Identification Rate
Kind 7 = Cropped and masked to facilitate compression **FPIR** = False Positive Identification Rate

381 **4.1.2 Quantization Step Size**

382 **Introduction**

383 After the wavelet transform, the coefficients are quantized to reduce the number of bits required to represent them. Quan-
 384 tization can introduce rounding and truncation error. The amount of quantization is determined by a step size parameter,
 385 where larger values correspond to finer granularity (i.e. greater precision and fidelity to the original image), but require
 386 more bits to represent. A different step size can be specified for each tile and decomposition level, but since there are no
 387 obvious theoretical benefits to doing so, this study only measures the effect of varying a single global value. This value is
 388 appropriately scaled according to the resolution of the decomposition level. A small step size is often recommended since
 389 quantization is a lossy procedure, and selective retention of information should be handled primarily by the entropy coder.
 390 Kakadu's default value is 1/256, which is quite small.

391 **Results and Recommendations**

392 Figure 6 shows recognition accuracy as a function of file size when search images are compressed with different step sizes.
 393 All other compression parameters are left at their default values. The figure demonstrates a clear benefit to using smaller
 394 step sizes when the file size is larger (≥ 2048 bytes), although the benefit diminishes at smaller file sizes. Step sizes 1/256
 395 and 1/64 yield nearly identical results. We recommend using a step size of 1/256 because small step sizes never seem to
 396 perform worse than larger ones, and because it is a commonly used value.

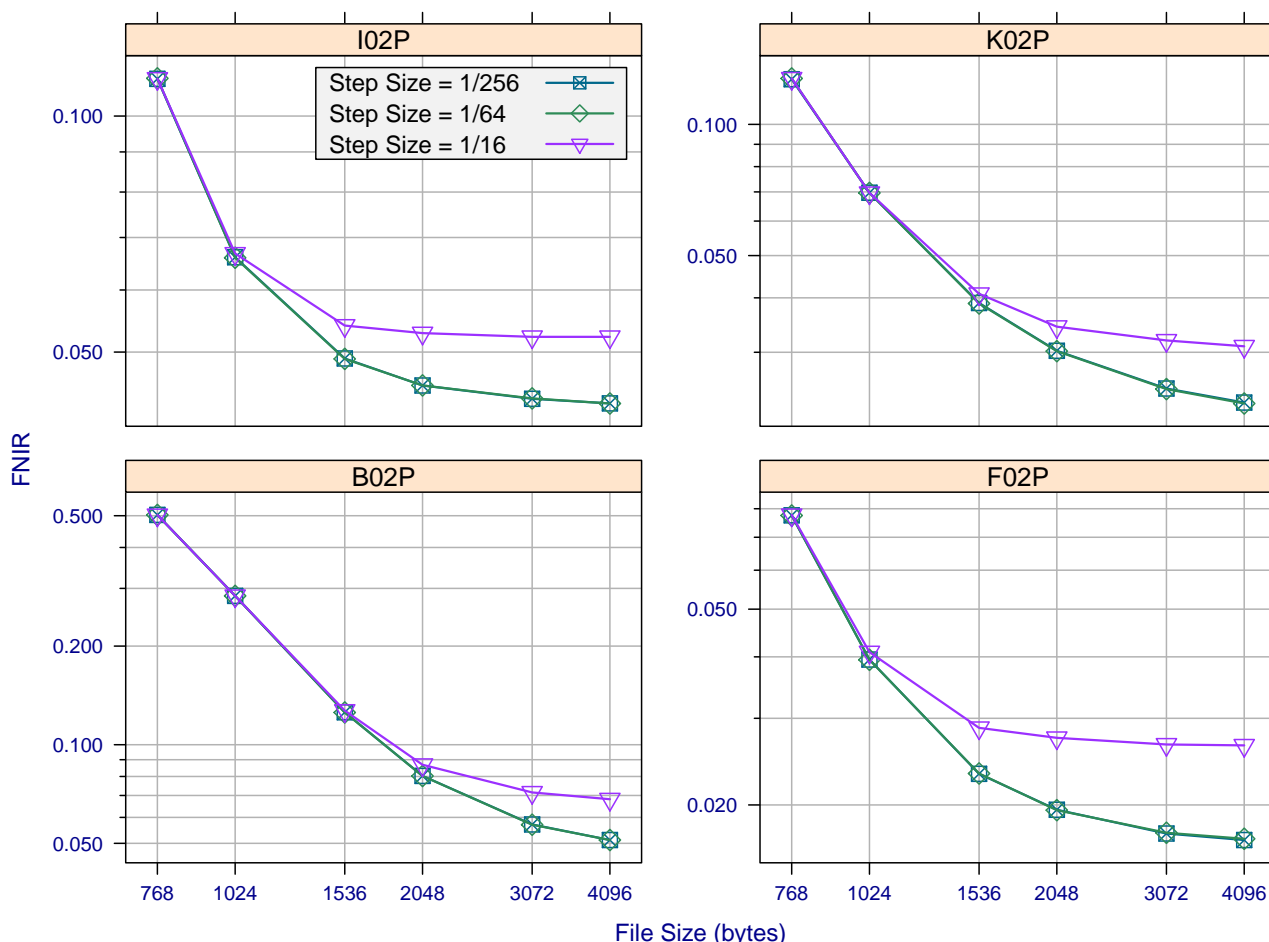


Figure 9: FNIR (at FPIR=0.001) as a function of file size for 4 matching algorithms when search images are compressed at different base step sizes. Compressed Kind 7 records (created by the matching algorithms) are searched against an enrolled population of 160 000 non-compressed images. Each point is generated from 80 135 mated searches.

397 **4.1.3 Number of Decomposition Levels**

398 **Introduction**

399 The wavelet transform decomposes the image into a number of different resolution levels. The process has been shown to
 400 work well for wavelet-based compression techniques. A further advantage of separating the image into multiple resolution
 401 levels is that the image can be re-constructed up to a certain resolution by only decompressing those levels that correspond
 402 to the lower frequencies. This can save time when rendering images on low-resolution embedded devices.

403 **Results and Recommendations**

404 Figure 10 shows recognition accuracy as a function of file size when search images are compressed with different numbers
 405 of decomposition levels. All other compression parameters are left at their default values (i.e. a single tile, a quantization
 406 step size of 1/256, and a block size of 64). Performance tends to be poorest when only one decomposition level is used. At
 407 small file sizes (≤ 1024), 3 decomposition levels always yield the best performance for all recognition algorithms. Thus, we
 408 recommend setting the number of decomposition levels to 3 when compressing iris images.

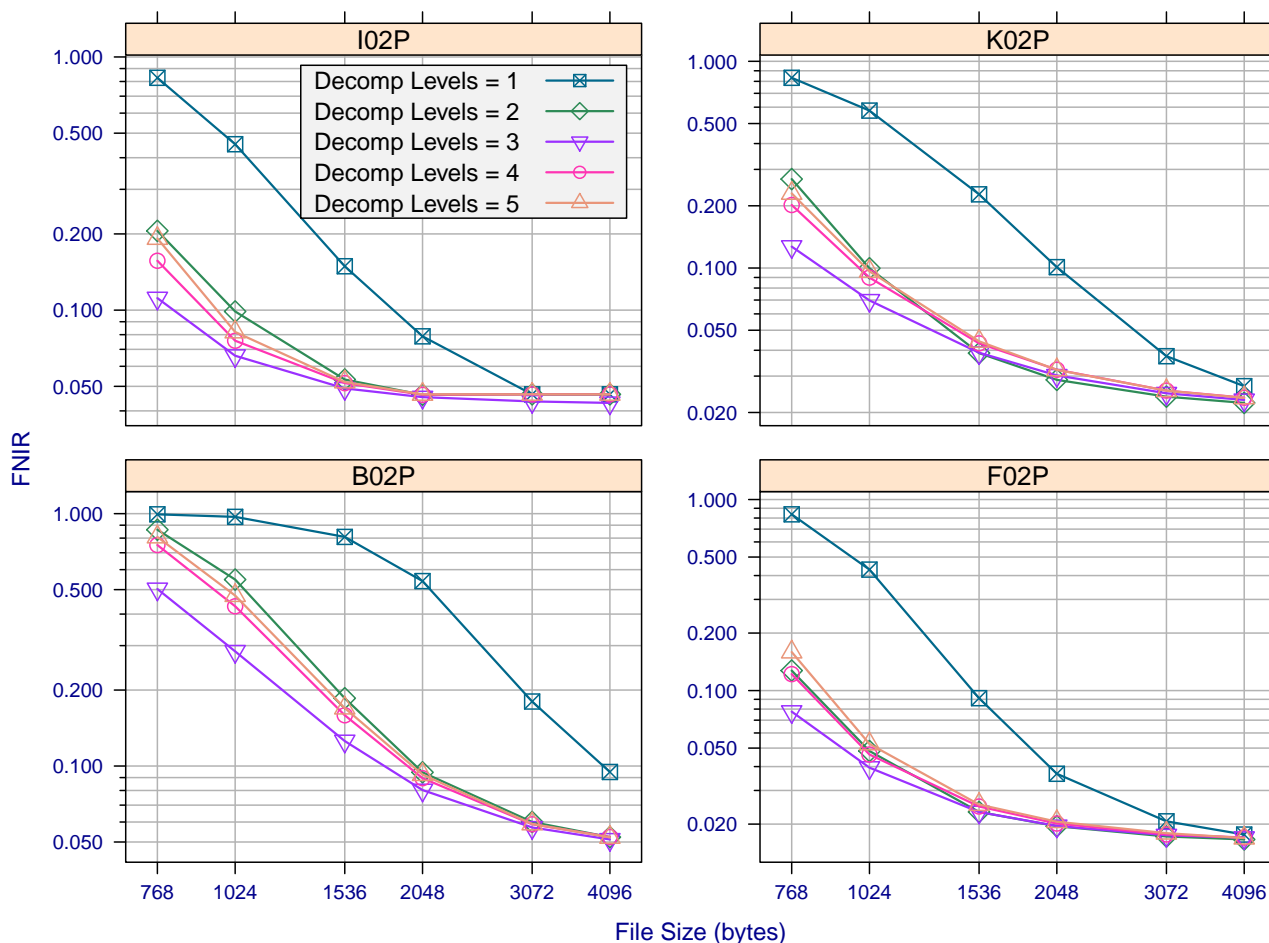


Figure 10: FNIR (at FPIR=0.001) as a function of file size for 4 matching algorithms when search images are compressed using different numbers of decomposition levels. Compressed Kind 7 records (created by the matching algorithms) are searched against an enrolled population of 160 000 non-compressed images. Each point is generated from 80 135 mated searches.

409 **4.1.4 Block Size**

410 **Introduction**

411 Each decomposition level is further divided into code blocks. Code blocks are encoded as bit-streams, with the most
 412 important bits located earlier in the stream. Since each code-block is coded independently of the others, a multi-threaded
 413 machine can encode blocks in parallel, saving computation time. The entropy coder operates directly on these blocks,
 414 truncating each at a point that minimizes the overall squared error loss. The code block size is normally set to either 32-by-
 415 32 or 64-by-64. These dimensions refer to the number of wavelet coefficients in the vertical and horizontal directions, both
 416 of which must be powers of 2. We see no obvious reason to test non-square dimensions given the properties of iris images.
 417 Since the total number of coefficients cannot exceed 4 096, this restricts the block size to no more than 64-by-64.

418 **Results and Recommendation**

419 Figure 11 shows recognition accuracy as a function of file size when search images are compressed using different code-
 420 block sizes. All other compression parameters are left at their default values. Performance is poorest for block sizes of only
 421 8-by-8. The difference between code blocks of 32-by-32 and 64-by-64 is too small to establish statistical significance. For
 422 the sake of consistency, we recommend setting this value to 64-by-64.

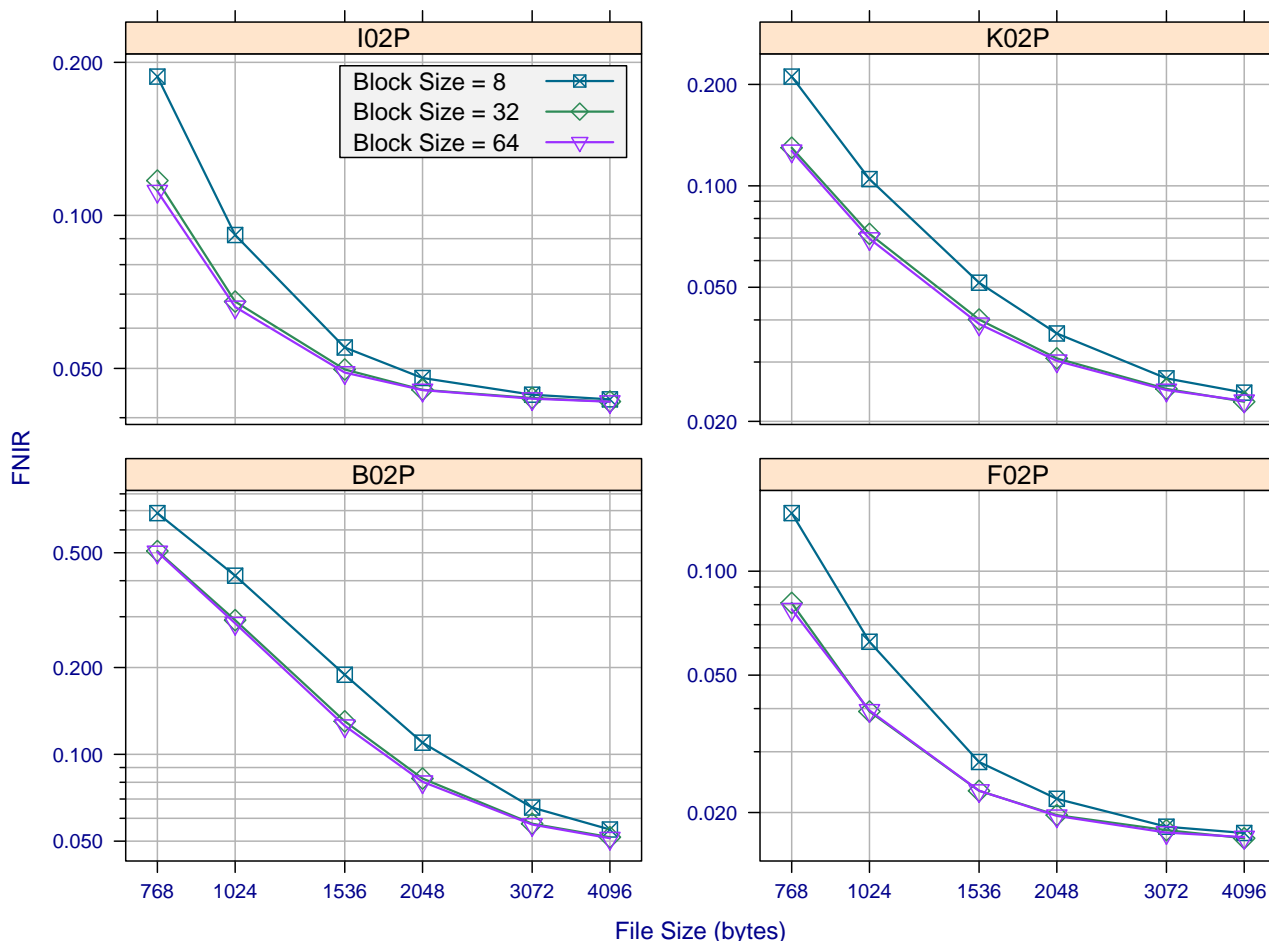


Figure 11: FNIR (at FPIR=0.001) as a function of file size for 4 matching algorithms when search images are compressed using different code-block sizes. Compressed Kind 7 record (created by the matching algorithms) are searched against an enrolled population of 160 000 non-compressed images. Each point is generated from 80 135 mated searches.

4.1.5 Timing Statistics

The time it takes to compress an iris image can be an important performance factor, especially on computationally limited devices. Figure 12 shows the distribution of compression times when Kind 2 and Kind 7 records are compressed to various file sizes. Parameters such as tile and block size are set to optimal values listed in Section 4.1.6. Section 3.5.3 describes the procedure for collecting timing statistics and Section 3.1 outlines the specifications of the timing machine, a high-end PC class blade with 6 quad-core AMD Opteron CPUs running at 2.4 GHz.

Although the targeted file size does not significantly affect compression time for Kind 7 records, Kind 2 records take longer to compress at larger file size. Generally speaking, Kind 2 records take longer to compress than Kind 7 records, possibly because the former have larger pixel dimensions and contain additional textures. Compression takes an average of 0.014 seconds for Kind 7 records, which is small compared to other steps performed during identification. Some recognition algorithms are capable of creating matching templates in as little as 3 hundredths of a second, but others require half a second or longer on a timing machine with identical specifications (see the IREX IV: Part 1 Final Report). Searching a template against an enrolled population of 1.6 million irides can take anywhere from half a second to half a minute, depending on the recognition algorithm.

Figure 13 shows the distribution of compress times when Kind 7 records are compressed with different numbers of processing threads and block sizes. Sometimes the median compression time equals the 10th or 90th percentile because the timer has only millisecond resolution. Dedicating more threads to compression does not improve end-to-end compression time, possibly because the overhead of loading software libraries, which can only be done with a single thread, dominates execution time. Median compression time is sometimes lowest when only one thread is used. Only certain steps of the compression process can utilize multiple threads. One such step is code blocking, which is performed immediately prior to EBCOT encoding. Since iris records are fairly low resolution images that compress quickly, it may be that multithreading incurs an overhead greater than the benefit of coding blocks concurrently. Compressing with a block size of only 8-by-8 appears to increase computation time. Otherwise, there is no pronounced difference in computation time for block sizes of 32-by-32 and 64-by-64.

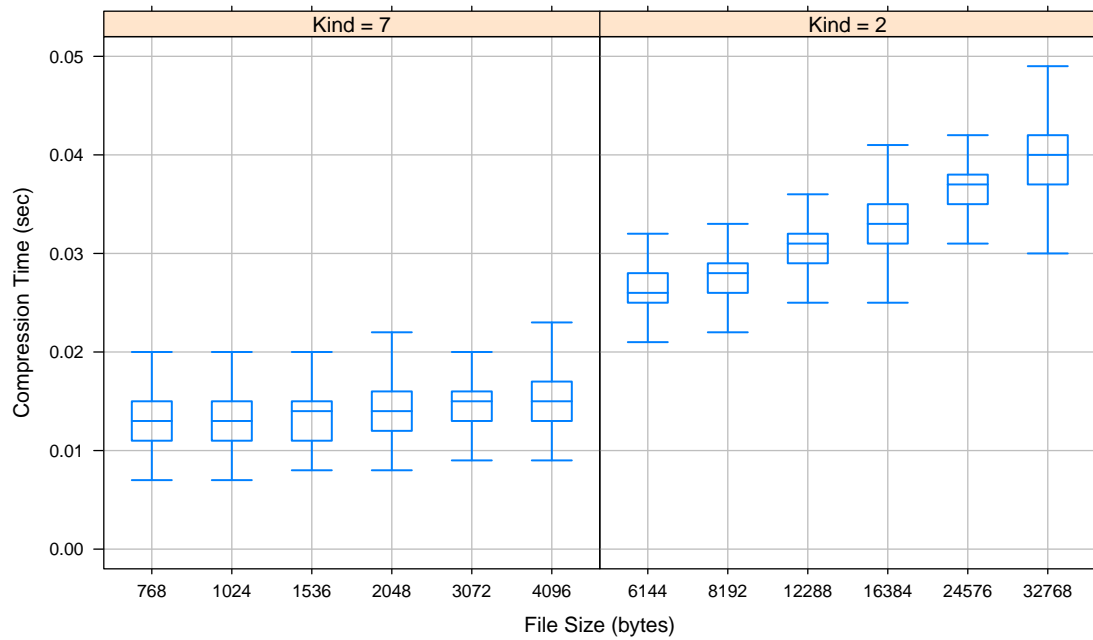


Figure 12: Distribution of compression times when Kind 2 and Kind 7 records are compressed to various file sizes on an otherwise unloaded high-end machine with 6 quad-core AMD Opteron processors operating at 2.4 GHz. Each plot is generated from compressing 5 000 images. The resolution of the timer is 0.001 seconds (rounded).

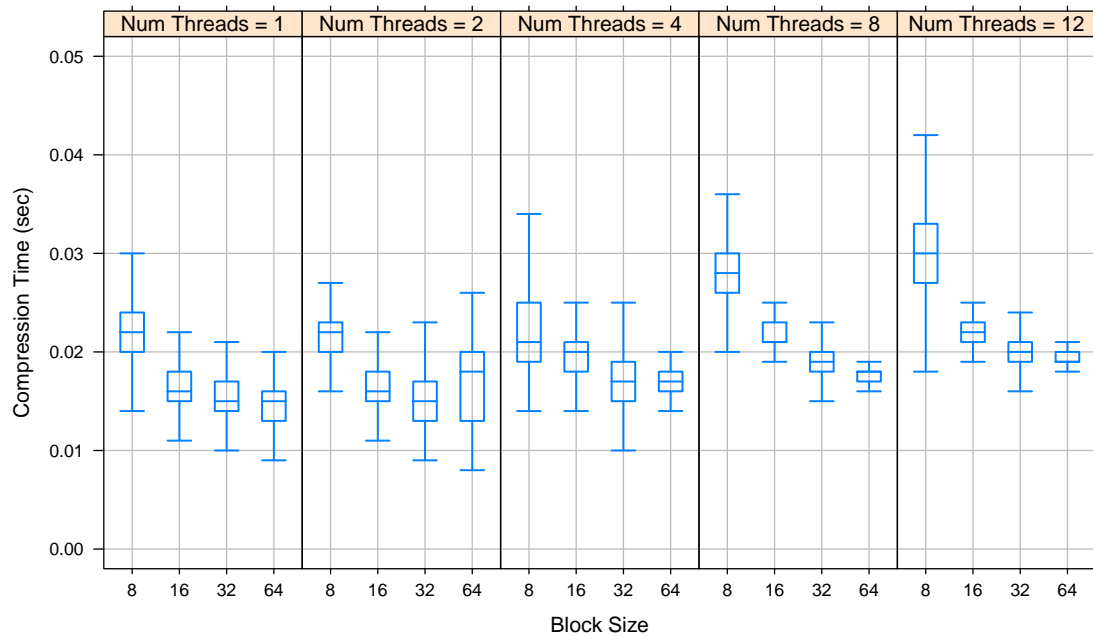


Figure 13: Distribution of compression times for Kind 7 records when different numbers of processing threads and block sizes are used. Block sizes are always square. Images are always compressed to 3 072 bytes. Each plot is generated from compressing 5 000 images. The resolution of the timer is 0.001 seconds (rounded).

4.1.6 Summary of Recommendations

The following parameter values were found to produce the smallest drop in recognition accuracy:

- a single tile,
- a block size of 64-by-64,
- a quantization step size of $1/256$.
- 3 decomposition levels.

At small file sizes (e.g. those below 2048 bytes), recognition accuracy is especially sensitive to the number of tiles and the number of decomposition levels. At larger file sizes, recognition accuracy is more sensitive to the quantization step size. The best combination of parameters does not change depending on the file size.

4.2 Performance of Kind 7 Format

This section explores the effect of lossy compression on Kind 7 records. The Kind 7 format is the most compact format for storing iris images described in ISO/IEC 19794-6. The standard requires the iris to be centered in the image, and the superfluous area around the iris to be cropped and masked. The masking ensures that a maximum of the encoding budget is dedicated to representing the iris features rather than less relevant periocular textures.

Iris images are compressed to fixed file sizes to address applications that impose a hard upper-limit on the container size. Since Kind 7 records can vary in pixel dimensions, the bit rate (in bits-per-pixel) input to the compression software had to be adjusted for each image to correspond to the correct file size. Sometimes the image is a few bytes smaller than the targeted file size, but it is never greater.

4.2.1 Compressing Only Search Images

Applications

Some setups may only require compression of images on one side of the comparison process. Systems that compare compressed samples from digital smartcards to live captures often have no need to compress the live captures, especially when they only need to exist for the duration of the transaction. Systems that transfer compressed samples across bandwidth-limited networks may search these samples against previously enrolled samples that were never compressed. The results in this section are more closely related to the latter example since images are only compressed on the search side.

Results

Figure 14 shows DET accuracy when Kind 7 records are compressed to different file sizes and searched against an enrolled population of 160 000. Compression parameters such as block size and step size are set to optimal values identified in Section 4.1.6. Line segments connect *points of equal threshold* between curves, which show the specific effect that compression has on the mated and non-mated comparison score distributions. The following conclusions are drawn from the figure:

- Compressing search images down to 2048 bytes results in only a small drop in accuracy ($\sim 1/3$ increase in FNIR at fixed FPIR) for algorithms I02P and F02P. Algorithm B02P experiences a greater decrease in accuracy (about a factor of 10 increase in FNIR at fixed FPIR) since it fails to mask the sclera.
- Accuracy drops much more appreciably when search images are compressed to 1024 bytes. At fixed FPIR, FNIR increases by about a factor of 2 for I02P, a factor of 3 for F02P, a factor of 5 for K02P, and more than 10 for B02P.
- High amounts of compression decrease non-mated dissimilarity scores for algorithms I02P and B02P. In the case of I02P, the increase in FPIR at a fixed threshold is approximately 4 fold when search images are compressed to 1024 bytes. The increase is much larger for B02P. Algorithms F02P and K02P do not exhibit appreciable increases in FPIR.

Operational Relevance

Algorithms that mask the sclera and blur the eyelid boundaries achieve noticeably superior accuracy when images are compressed to small file sizes ($\leq 3,072$ bytes). Kind 7 records can be compressed to sizes as small as 2048 bytes with only minor degradation in recognition accuracy. Accuracy drops much more quickly when search images are compressed to sizes smaller than 2048 bytes. Compared to other biometric modalities, standard fingerprint minutiae information can be

491 stored in as little as 400 bytes [8]. and face images can be compressed to about 8KB [27], although the ISO/IEC 19794-5
492 standard [28] recommends 30KB to be safe.

493 High amounts of compression tend to increase dissimilarity scores for mated comparisons. High amounts of compression
494 sometimes decrease dissimilarity scores for non-mated comparisons, but to a lower extent. Sometimes it may be advanta-
495 geous to adjust the decision threshold depending on the amount of compression applied to the images.

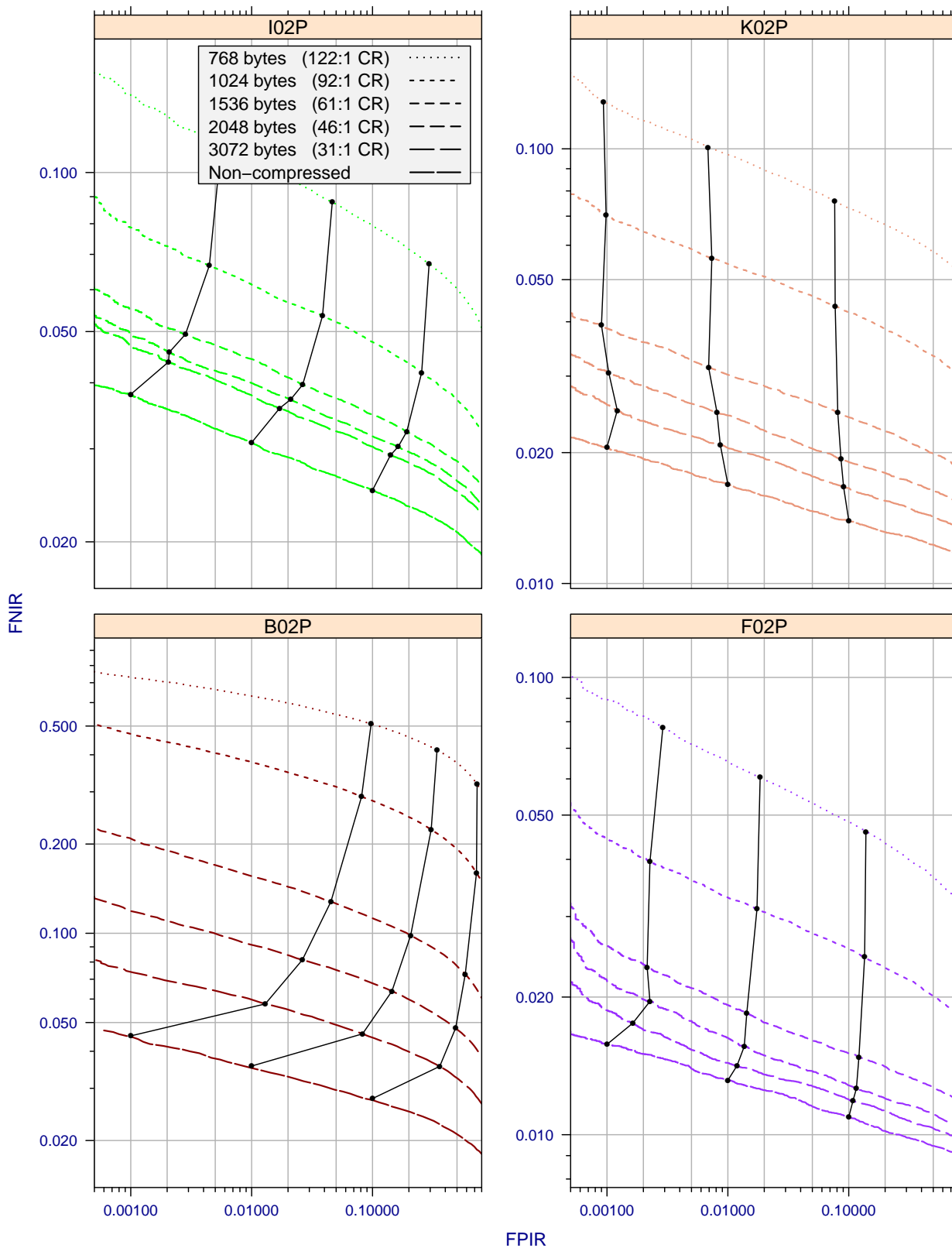


Figure 14: DET accuracy when Kind 7 records are compressed to different file sizes and searched against an enrolled population of 160 000. Enrolled images were never compressed. Line segments connect points of equal threshold. The mean compression ratio corresponding to each file size is included in the legend. Plots are generated using 80 135 mated and 60 000 non-mated searches.

Kind 2 = Unprocessed from iris camera

Kind 7 = Cropped and masked to facilitate compression

FNIR = False Negative Identification Rate

FPIR = False Positive Identification Rate

496 4.2.2 Compressing Search and Enrollment Images

497 Applications

498 Some iris recognition systems may match compressed images against other compressed images. Systems that must
499 transfer both the smartcard sample and the live capture across a network are likely to compress both. A setup was described
500 in Section 4.2.1 where compressed iris samples are transferred and searched against a back-end database of enrolled
501 samples. After a positive identification is made, the system may opt to replace the sample on the enrollment side with the
502 newly acquired (and compressed) sample that it matched.

503 Results

504 Figure 15 shows DET accuracy when Kind 7 search and enrollment images are similarly compressed to targeted file sizes.
505 The enrolled population is 160 000. Compression parameters such as block size and step size are set to optimal values
506 identified in Section 4.1.6. Lines segments connect *points of equal threshold* between curves, which show the specific effect
507 that compression has on the mated and non-mated comparison score distributions. The following conclusions are drawn
508 from the figure:

- 509 • Accuracy is similar to when only the search images are compressed. Compression sizes of 2 048 bytes result in only
510 a small drop in accuracy ($\sim 1/5$ factor increase in FNIR at fixed FPIR) for algorithms I02P and F02P. Algorithm B02P
511 experiences a greater decrease in accuracy (about a factor of 10 increase in FNIR at fixed FPIR) since it fails to mask
512 the sclera.
- 513 • Accuracy drops much more appreciably when images are compressed to sizes smaller than 2 048 bytes. At fixed
514 FPIR and a compression size of 1 024 bytes, FNIR increases by about a factor of 2 for I02P, a factor of 2.5 for F02P, a
515 factor of 4.5 for K02P, and more than 20 for B02P.
- 516 • High amounts of compression increase non-mated dissimilarity scores for algorithms I02P and B02P, but to a lesser
517 extent than if only search images had been compressed (determined by comparing these results to Figure 14). In the
518 case of I02P, the increase is minor (no more than a factor of 3 increase in FPIR at fixed threshold when images are
519 compressed to 1 024 bytes). Algorithms F02P and K02P do not experience appreciable increases in FPIR.

520 Operational Relevance

521 Results are similar to when only search images are compressed. Algorithms that mask the sclera and blur the eyelid
522 boundaries achieve noticeably superior accuracy when images are compressed to small file sizes ($\leq 3,072$ bytes). Kind 7
523 records can be compressed to sizes as small as 2 048 bytes with only minor degradation in recognition accuracy. Accuracy
524 drops much more quickly when images are compressed to sizes smaller than 1 536 bytes. High amounts of compression tend
525 to increase dissimilarity scores for mated comparison. Dissimilarity scores for nonmated comparisons decrease somewhat
526 for some algorithms, but to a lesser extent than when both images are compressed.

527 Lossy compression discards potentially identifying information. While it is preferable to discard as little information as possible,
528 compressing enrolled images by an amount comparable to search images does not lead to an appreciable drop in
529 accuracy. This may be because compression tends to discard similar feature information in both images, and iris matchers
530 benefit mostly from feature information only when it is present in both images.

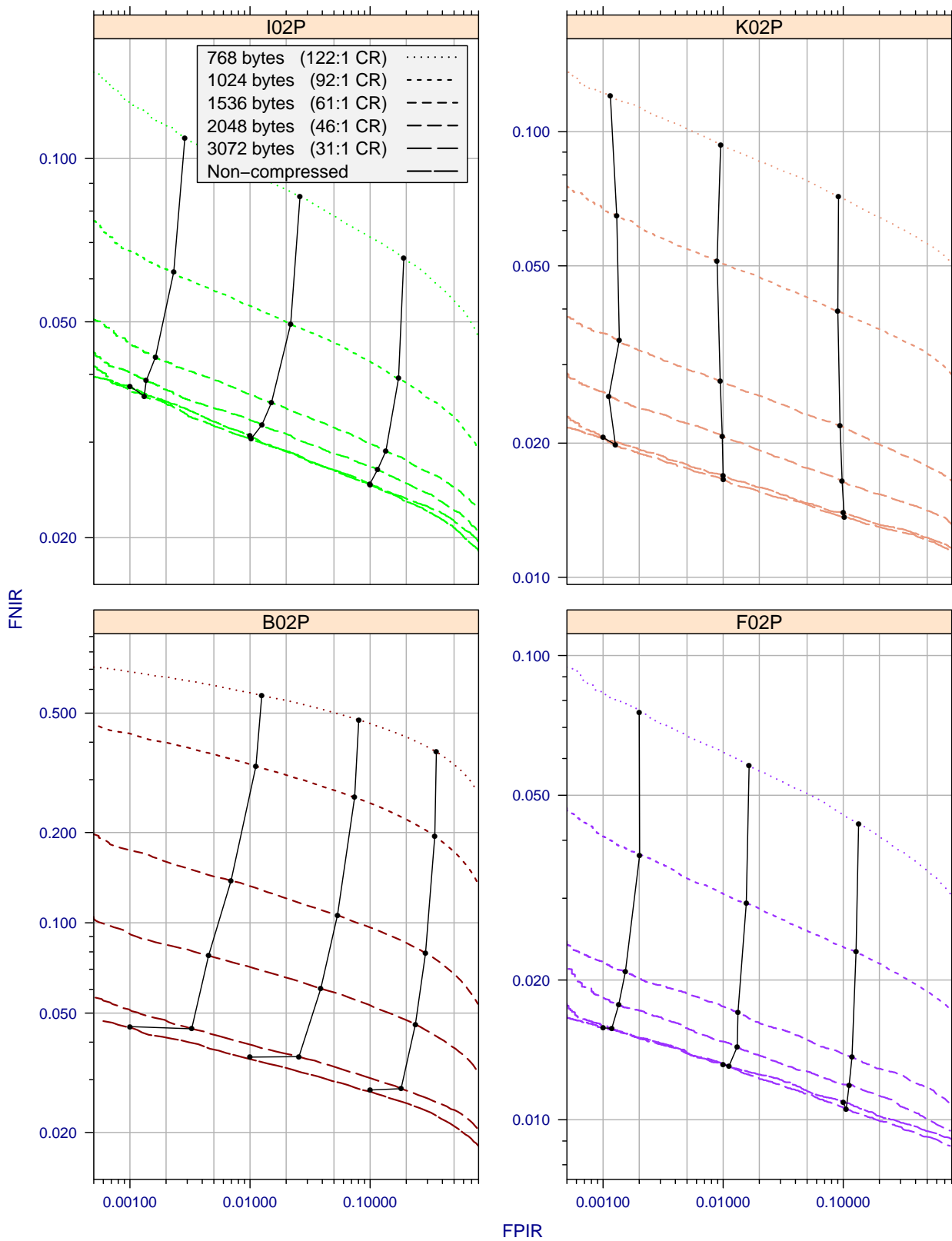


Figure 15: DET accuracy when Kind 7 records are compressed to different file sizes. The size of the enrollment population is 160 000. Both search and enrollment images are compressed. Line segments connect points of equal threshold. The mean compression ratio corresponding to each file size is included in the legend. Plots were generated using 80 135 mated and 60 000 non-mated searches.

Kind 2 = Unprocessed from iris camera

Kind 7 = Cropped and masked to facilitate compression

FNIR = False Negative Identification Rate

FPIR = False Positive Identification Rate

531 **4.2.3 When to use Both Eyes**

532 **Applications**

533 If the goal is to maximize recognition accuracy, images of both eyes should be used for matching whenever available.
 534 However, if only a fixed amount of storage space is available, the question becomes whether better accuracy is achieved
 535 by storing images of both eyes, or a more lightly compressed version of just one. Part 1 of the IREX IV report found that
 536 using both eyes results in only about a factor of 3 to 4 reduction in FNIR at fixed FPIR, which is indicative of a high degree
 537 of positive correlation between left and right eyes captured during the same session. This makes sense since people tend
 538 to blink or look off to the side simultaneously with both eyes. Unfortunately, it diminishes the benefit to using both eyes for
 539 matching.

540 **Results and Recommendations**

541 Figure 16 shows recognition accuracy as a function of file size when searches are performed with one eye, and with two
 542 eyes. Compression parameters such as tile and block size are set to optimal values identified in Section 4.1.6. Only search
 543 images are compressed. The figure demonstrates that there is a crossover point, where one-eye matching is more accurate
 544 at lower storage capacities, but less accurate than two-eye matching at larger storage capacities. The crossover tends to
 545 occur between 2 and 3KB. At sizes of 1.5KB, one-eye matching is consistently more accurate. At 4KB or more, two-eye
 546 matching is usually more accurate. Note that matching with two eyes introduces an additional computation penalty that may
 547 offset possible accuracy benefits.

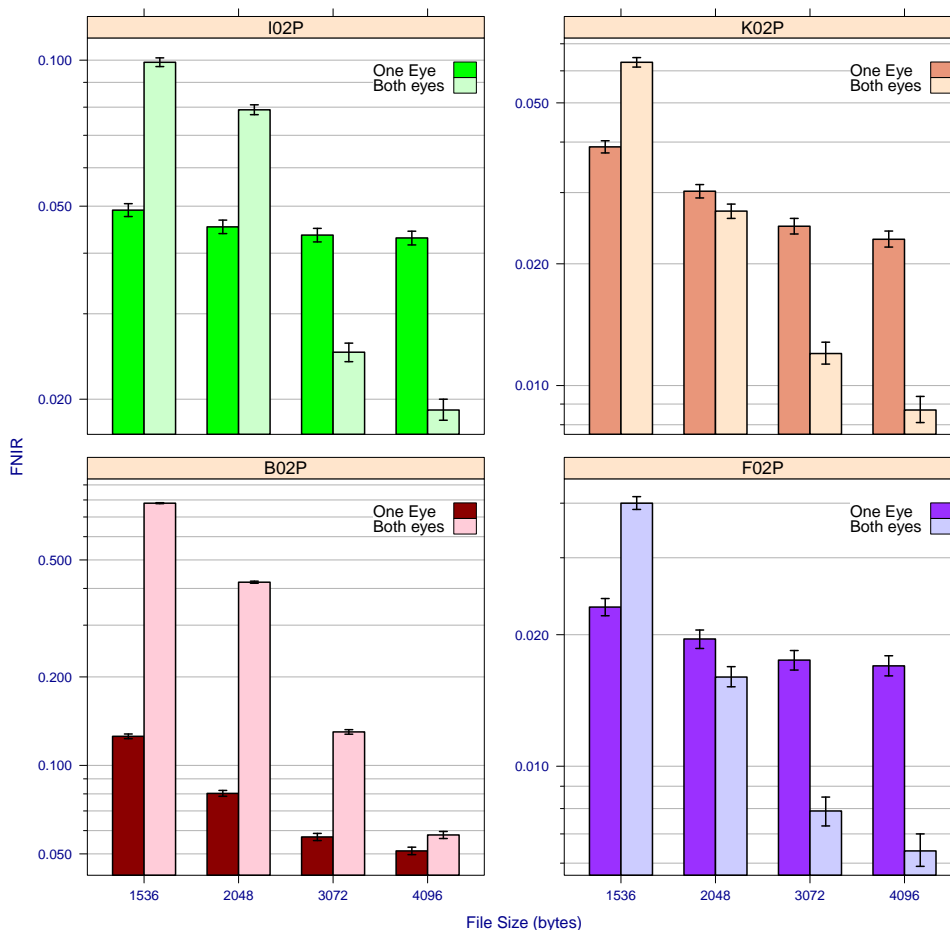


Figure 16: Comparison of FNIR (at an FPIR of 0.001) for one-eye and two-eye matching at different maximum storage capacities. Only search images are compressed. Each point is generated from 80 135 mated searches and 60 000 nonmated searches against an enrolled population of 160 000.

548 4.2.4 Should Images be Downsampled?

549 Introduction

550 Downsampling an image's pixel resolution prior to performing compression may improve recognition accuracy when the
551 amount of compression is high. Downsampling selectively discards the highest frequency information in the image. If this
552 information is less important for matching, then ensuring that it is discarded during the compression procedure may improve
553 recognition accuracy. Extending this line of thinking a bit further, an optimal combination of resolution downsampling and
554 JPEG 2000 compression could be identified that selectively retains the frequency ranges most important for matching.
555 However, over-tuning of the compression procedure runs the risk of compromising interoperability, especially since not all
556 recognition algorithms use precisely the same features for matching.

557 Two methods of downsampling are tested in this study. The first involved simple 2x2 pixel averaging. The downsampled
558 image is then passed to the JPEG 2000 compression algorithm. The compressed image is then decompressed and up-
559 scaled to its original size before it is passed to the matcher. Upscaling is performed via bilinear interpolation. The second
560 method of downsampling simply instructs the Kakadu implementation to allocate no space to representing the highest
561 frequency information in the image. This has a roughly similar effect to 2x2 pixel averaging, but allows the step to be
562 performed directly by the JPEG 2000 encoder. One would also expect the JPEG 2000 encoder to do a better job of
563 minimizing the mean square error loss subject to the given constraint.

564 A similar study on automated face recognition [27] concluded that downsampling provided no perceivable accuracy benefit
565 since JPEG 2000 already preferentially discards the higher frequency information during compression.

566 Results and Recommendations

567 Figure 17 compares recognition accuracy when different methods of compression are applied to search images. Compres-
568 sion parameters such as tile and block size are set to optimal values identified in Section 4.1.6. Results are inconsistent
569 across algorithms, and no single method of compression works best in all cases. Reducing the image resolution through
570 Kakadu achieves the best results for algorithms I02P and F02P, and at compression sizes ≥ 2048 for algorithm K02P. How-
571 ever, the improvement is sometimes so small that it may not be statistically significant. Furthermore, whenever downsampling
572 appears to offer a benefit, the fractional drop in FNIR remains almost constant over the full range of file sizes. One would
573 expect the performance disparity to be greater at smaller file sizes. More likely, downsampling is removing some type of
574 noise (e.g. camera shot noise) that leads to the improvement.

575 Neither method of downsampling results in a consistent improvement in recognition accuracy. Many other methods of
576 decimation and/or filtering are possible, and some may reap clear benefits. Although further investigation is warranted,
577 downsampling cannot be recommended at this time.

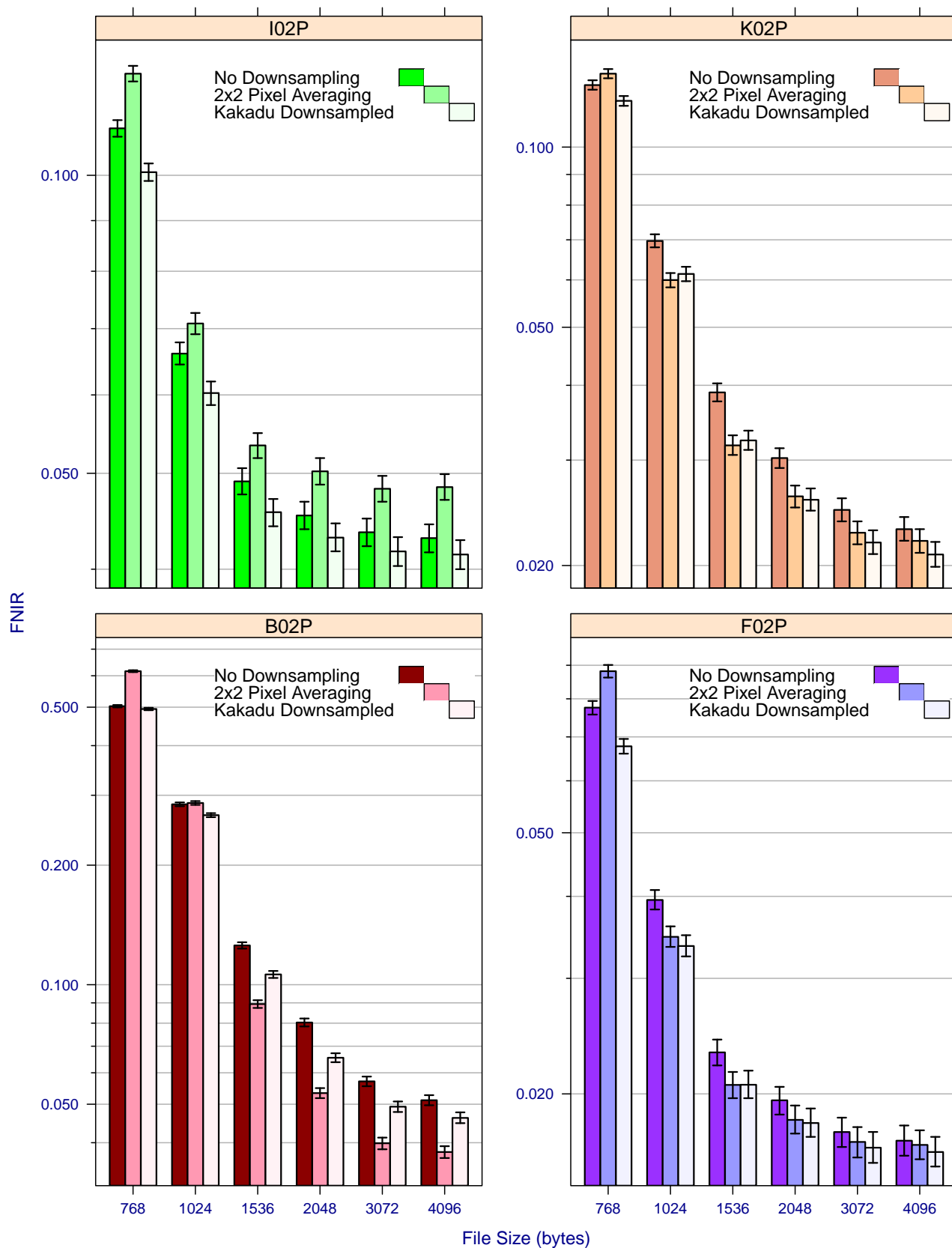


Figure 17: Comparison of FNIR (at FPIR=0.001) with and without downsampling applied to search images. 80 135 searches are performed against an enrolled population of 160 000 (non-compressed) iris images. Error bars show 95% confidence intervals.

Kind 2 = Unprocessed from iris camera

Kind 7 = Cropped and masked to facilitate compression

FNIR = False Negative Identification Rate

FPIR = False Positive Identification Rate

578 4.3 Performance of Kind 2 Format

579 Kind 2 records must have pixel dimensions of 640x480 and a bit depth of 8, but otherwise do not require a masking or
580 cropping of the area outside the iris. As such, they cannot be compressed to sizes as small as Kind 7 records without
581 suffering much greater losses in accuracy. Iris cameras typically return Kind 2 images, so no additional processing is
582 required to create them. Creating Kind 7 records, on the other hand, requires localization of the iris center as well as the
583 limbus and eyelid boundaries, which is a non-trivial task.

584 4.3.1 Compressing Only Search Images

585 Introduction

586 When file size constraints are more relaxed, it may not be necessary to convert Kind 2 records into more compact Kind 7 rep-
587 resentations. Doing so requires localization of the limbus and eyelid boundaries, often on the client side where computational
588 resources may be limited.

589 Results and Recommendations

590 Figure 18 shows DET accuracy when Kind 2 are compressed to different file sizes and searched against an enrolled popu-
591 lation of 160 000. Compression parameters such as block and step size are set to optimal values identified in section 4.1.6.
592 Line segments connect *points of equal threshold* between curves, which shows the specific effect that compression has on
593 the mated and non-mated comparison score distributions. The following conclusions are drawn from the figure:

- 594 • Compressing search images down to 16 384 bytes results in only a moderate to small drop in accuracy ($< 1/3$
595 increase in FNIR at fixed FPIR) for all algorithms.
- 596 • Accuracy drops more appreciably when search images are compressed to 8 192 bytes. At fixed FPIR, FNIR increases
597 by about a factor of 2 for I02P and K02P, and a bit more than a factor of 2 for B02P and F02P. At 6 144 bytes, the factor
598 increase in FNIR ranges from about 2.5 to 4 depending on the algorithm.
- 599 • High amounts of compression decrease non-mated dissimilarity scores for algorithms I02P and B02P. In the case of
600 I02P, the increase in FPIR at a fixed threshold is no more than a factor of 5 when search images are compressed to
601 6 144. Algorithms F02P and K02P do not experience appreciable increases in FPIR.

602 Figure 19 compares the ability of iris recognition algorithms to match highly compressed Kind 2 and Kind 7 records. Kind 7
603 records typically perform better at file sizes under 16 384. At larger file sizes there appears to be little or no accuracy benefit
604 to matching Kind 7 records over their Kind 2 counterparts. Kind 7 records achieve the same FNIR as Kind 2 records at only
605 a fraction of the size. FNIR is comparable when file sizes are reduced by a factor of 5 for B02P and K02P, and a factor of 8
606 for I02P and F02P.

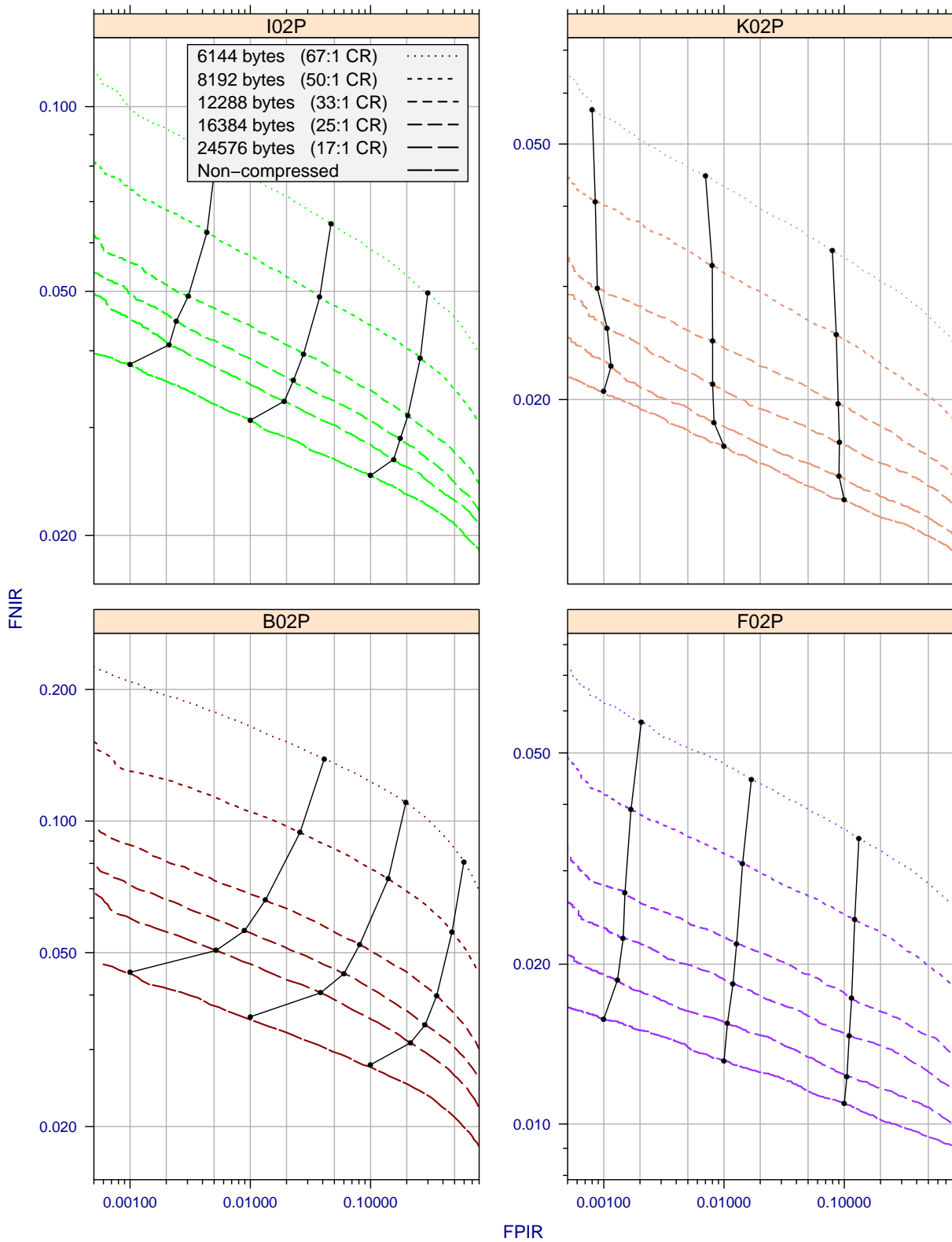


Figure 18: DET accuracy when Kind 2 records are compressed to different file sizes and searched against an enrolled population of 160 000. Enrolled images were never compressed. Line segments connect points of equal threshold. The compression ratio corresponding to each file size is included in the legend. Plots are generated using 80 135 mated and 60 000 non-mated searches.

Kind 2 = Unprocessed from iris camera

Kind 7 = Cropped and masked to facilitate compression

FNIR = False Negative Identification Rate

FPIR = False Positive Identification Rate

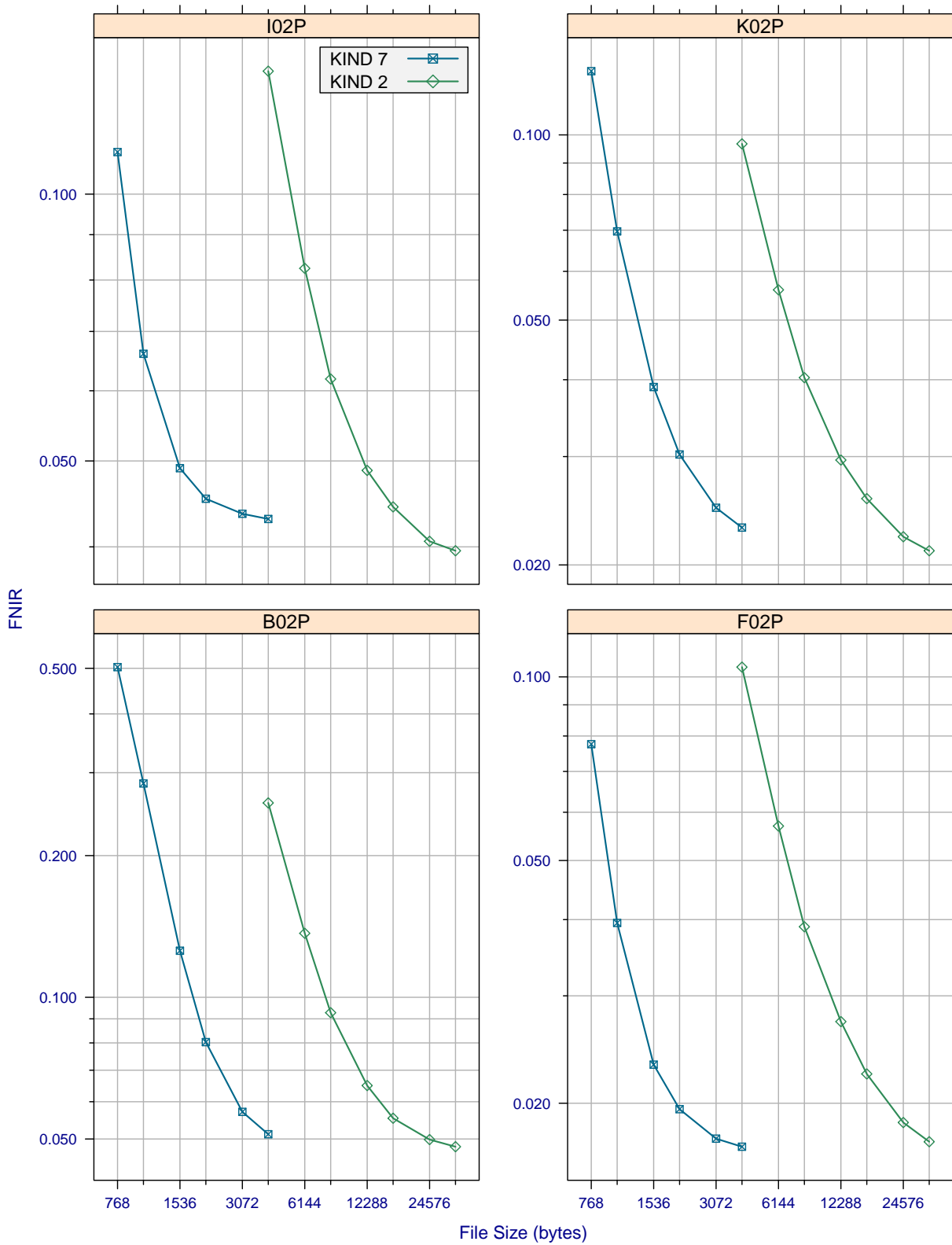


Figure 19: Comparison of FNIR (at FPIR=0.001) when Kind 2 and Kind 7 records are compressed to various file sizes and searched against an enrolled population of 160 000 non-compressed images. Each point is generated from 80 135 mated searches. Kind 7 records perform better at smaller file sizes because they undergo cropping and masking that allows them to be stored more compactly.

Kind 2 = Unprocessed from iris camera

Kind 7 = Cropped and masked to facilitate compression

FNIR = False Negative Identification Rate

FPIR = False Positive Identification Rate

607 4.3.2 Compressing Search and Enrollment Images

608 Introduction

609 Some iris recognition systems may match compressed Kind 2 records against other compressed iris records. Possible
610 setups are described in Section 4.2.2.

611 Results and Recommendations

612 Figure 20 shows DET accuracy when Kind 2 search and enrollment images are similarly compressed to targeted file sizes.
613 The size of the enrolled population is 160 000. Compression parameters such as block and step size are set to optimal values
614 identified in section 4.1.6. Line segments connect *points of equal threshold* between curves, which shows the specific effect
615 that compression has on the mated and non-mated comparison score distributions. The following conclusions are drawn
616 from the figure:

- 617 • Accuracy is similar to when only the search images are compressed. Compression sizes of 16 384 bytes result in
618 moderate drops in accuracy ($< 1/4$ increase in FNIR at fixed FPIR) for all algorithms.
- 619 • Accuracy drops more appreciably when search images are compressed to 8 192 bytes. At fixed FPIR, FNIR increases
620 by less than a factor of 2 for I02P, about a factor of 2 for F02P and K02P, and about a factor of 2.5 for B02P. At 6 144
621 bytes, the factor increase in FNIR ranges from about 2 to 4.5 depending on the algorithm.
- 622 • High amounts of compression increase non-mated dissimilarity scores for algorithms I02P and B02P, but to a lesser
623 extent than if only search images had been compressed (determined by comparing these results to Figure 18). In the
624 case of I02P, the increase is minor (no more than a factor of 3 increase in FPIR at fixed threshold when images are
625 compressed to 6 144 bytes). Algorithms F02P and K02P do not experience appreciable increases in FPIR.
- 626 • Light compression appears to actually improve performance for all algorithms. For algorithms I02P and K02P, the
627 drop in FNIR at fixed FPIR is almost $1/3$ when images are compressed to 24 576 bytes. The compression may be
628 removing some type of noise (e.g. shot noise) from the images. Lightly compressing iris images for the sole purpose
629 of improving accuracy is not recommended since these results may not translate to other iris data. Furthermore, such
630 processing should be handled internally by the recognition algorithm.

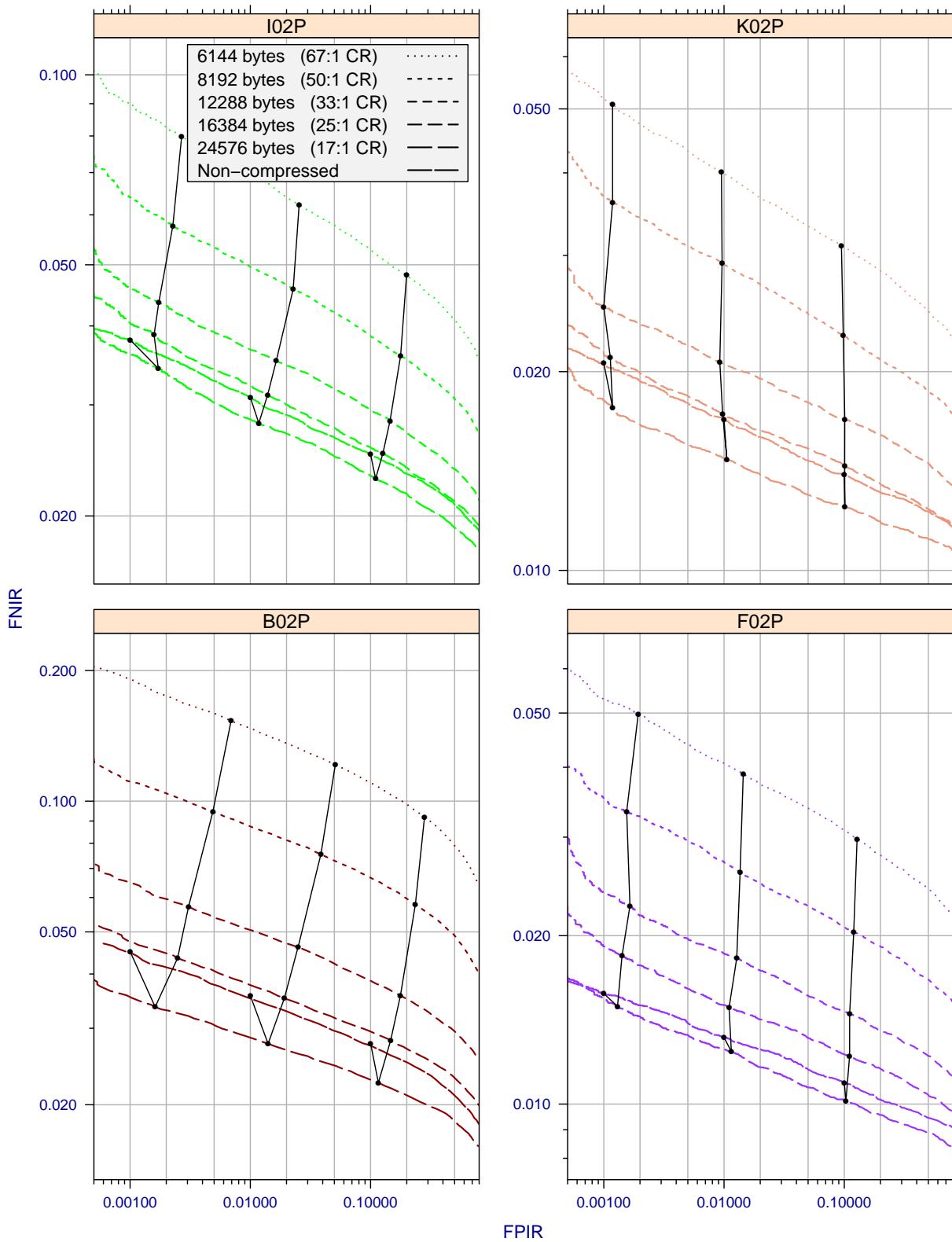


Figure 20: DET accuracy when Kind 2 search and enrollment images are similarly compressed to targeted file sizes. The size of the enrolment population is 160 000. Line segments connect points of equal threshold. The compression ratio corresponding to each file size is included in the legend. Plots are generated using 80 135 mated and 60 000 non-mated searches.

Kind 2 = Unprocessed from iris camera

Kind 7 = Cropped and masked to facilitate compression

FNIR = False Negative Identification Rate

FPIR = False Positive Identification Rate

631 4.4 Lossless Compression

632 Introduction

633 JP2 can compress images losslessly. Lossless compression retains all of the information in the image so that it can be
 634 perfectly reconstructed to its original form. Since no information can be discarded, it cannot achieve file sizes as small as
 635 when lossy compression is used. Smaller sizes can still be achieved by converting the image to a Kind 7 before compressing
 636 it since they have smaller pixel dimensions and uniform areas of solid color that are easy to represent compactly. Lossless
 637 compression requires the use of the 5/3 CDF wavelet transform.

638 Results

639 Figure 21 shows the distribution of file sizes achieved when images are compressed losslessly in their original Kind 2 format,
 640 and when they are converted to Kind 7 formats by 4 different algorithms. Kind 2 images compress to a mean size of 135KB.
 641 Algorithms I02P and F02P achieve the lowest file sizes for Kind 7 images since they mask the sclera and blur the eyelid
 642 boundaries. The mean file sizes are 20KB and 21KB for algorithms I02P and F02P respectively. An alternative lossless
 643 compression format is PNG. The IREX I Final Report found that libpng [29] compresses Kind 7 records to a median size of
 644 25KB, and Kind 2 images to a median size of 150KB.

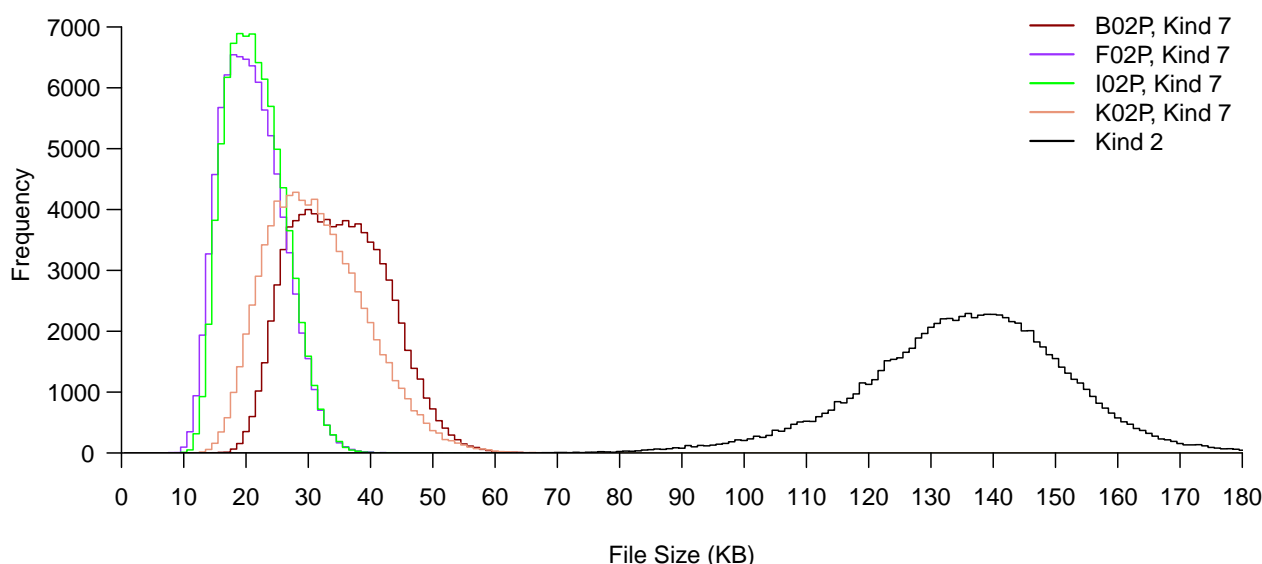


Figure 21: Distribution of file sizes when Kind 2 images, and Kind 7 images generated by different algorithms, are compressed losslessly. Each histogram is generated from 96 635 iris images.

645 **5 References**

- 646 [1] P. Grother, E. Tabassi, G. W. Quinn, and W. Salamon, "Performance of Iris Recognition Algorithms on Standard Images."
647 <http://www.nist.gov/itl/iad/ig/irex.cfm>, 2009. 1
- 648 [2] E. Tabassi, P. Grother, and W. Salamon, "IREX - IQCE Performance of Iris Image Quality Assessment Algorithms."
649 <http://www.nist.gov/itl/iad/ig/irexii.cfm>, 2011. 1
- 650 [3] *ISO/IEC 29794-6 - Biometric Sample Quality Standard- Part 6: Iris Image*. 2012. 1
- 651 [4] P. Grother, G. Quinn, J. Matey, M. Ngan, W. Salamon, G. Fiumara, and C. Watson, "IREX III: Performance of Iris
652 Identification Algorithms." <http://www.nist.gov/itl/iad/ig/irexiii.cfm>, 2011. 1
- 653 [5] P. Grother, J. R. Matey, E. Tabassi, G. W. Quinn, and M. Chumakov, "IREX VI: Temporal Stability of Iris Recognition
654 Accuracy." http://biometrics.nist.gov/cs_links/iris/irexVI/irex_report.pdf, 2013. 1
- 655 [6] "The IREX Program." <http://www.nist.gov/itl/iad/ig/irex.cfm>. 1
- 656 [7] "Special Publication 800-73-4 - Interfaces for Personal Identity Verification." [http://csrc.nist.gov/
657 publications/PubsDrafts.html](http://csrc.nist.gov/publications/PubsDrafts.html), 2013. 2
- 658 [8] *FIPS PUB 201-2: Personal Identity Verification (PIV) of Federal Employees and Contractors*. 2013. 2, 16
- 659 [9] "Registered Traveler Interoperability Consortium - Technical Interoperability Specification Version 1.7." [http://www.
660 rtconsortium.org/_docpost/RTICTIGSpec_v1.7.pdf](http://www.rtconsortium.org/_docpost/RTICTIGSpec_v1.7.pdf), 2008. 2
- 661 [10] "ICAO Doc 9303 - Machine Readable Travel Documents." [http://www.icao.int/publications/pages/
662 publication.aspx?docnum=9303](http://www.icao.int/publications/pages/publication.aspx?docnum=9303), 2008. 2
- 663 [11] "Prime Minister launches Aadhaar Enabled Service Delivery." Press Release, October 2012. [http://uidai.gov.
664 in/images/2nd_anniversary/uidai_press_release_for_oct_20.pdf](http://uidai.gov.in/images/2nd_anniversary/uidai_press_release_for_oct_20.pdf). 2
- 665 [12] *ISO/IEC 19794-6 - Biometric Data Interchange Formats - Iris Image Data*. 2011. 3
- 666 [13] *ANSI/NIST-ITL 1-2011 Data Format for the Interchange of Fingerprint, Facial & Other Biometric Information*. 2011. 3
- 667 [14] G. Quinn and P. Grother, "Irex iv: Evaluation of one-to-many iris recognition ,concept, evaluation plan, and api specifi-
668 cation." <http://www.nist.gov/itl/iad/ig/irexiv.cfm>, May 2012. 3
- 669 [15] P. J. Phillips, A. Martin, C. I. Wilson, and M. Przybocki, "An introduction to evaluating biometric systems," *Computer*,
670 vol. 33, pp. 56–63, Feb. 2000. 3
- 671 [16] G. Quinn and P. Grother, "IREX III Supplement I: Failure Analysis." [http://www.nist.gov/itl/iad/ig/
672 irexiii.cfm](http://www.nist.gov/itl/iad/ig/irexiii.cfm), 2011. 4
- 673 [17] D. Taubman, "Kakadu software version 7.0." [http://www.kakadusoftware.com/index.php?option=
674 com_content&task=view&id=56&Itemid=26](http://www.kakadusoftware.com/index.php?option=com_content&task=view&id=56&Itemid=26). 5
- 675 [18] *ISO/IEC 15444-1:2004 - Information technology – JPEG 2000 image coding system: Core coding system*. 2004. 5
- 676 [19] H. Drolon, F. Devaux, A. Descampe, Y. Verschuere, D. Janssens, and B. Macq, "OpenJPEG." [http://www.
677 openjpeg.org/](http://www.openjpeg.org/). 5
- 678 [20] M. D. Adams, "JASPER." <http://www.jpeg.org/jpeg2000/testlinks.html/>. 5
- 679 [21] "Nexus program description." [http://www.cbp.gov/xp/cgov/travel/trusted_traveler/nexus_
680 prog/nexus.xml](http://www.cbp.gov/xp/cgov/travel/trusted_traveler/nexus_prog/nexus.xml). 6
- 681 [22] A. Martin, G. Doddington, T. Kamm, M. Ordowski, and M. Przybocki, "The DET curve in assessment of detection task
682 performance," in *Proc. Eurospeech*, pp. 1895–1898, 1997. 6
- 683 [23] L. D. Brown, T. T. Cai, and A. Dasgupta, "Interval estimation for a binomial proportion," *Statistical Science*, vol. 16,
684 pp. 101–133, 2001. 7

- 685 [24] G. Doddington, W. Liggett, A. Martin, M. Przybocki, and D. Reynolds, "Sheep, goats, lambs and wolves a statistical
686 analysis of speaker performance in the nist 1998 speaker recognition evaluation," in *INTERNATIONAL CONFERENCE*
687 *ON SPOKEN LANGUAGE PROCESSING*, 1998. 7
- 688 [25] M. Antonini, M. Barlaud, P. Mathieu, and I. Daubechies, "Image Coding Using Wavelet Transform," *IEEE Transactions*
689 *on Image Processing*, vol. 1, no. 2, pp. 205–220, 1992. 8
- 690 [26] "Wellcome digital library." <http://wellcomelibrary.org/about-us/projects/digitisation/>. 9
- 691 [27] G. Quinn and P. Grother, "NIST Internal Report 7830: Performance of Face Recognition Algorithms on Compressed
692 Images." http://www.nist.gov/manuscript-publication-search.cfm?pub_id=908515, 2011.
693 16, 21
- 694 [28] *ISO/IEC 19794-5 - Biometric Data Interchange Formats - Face Image Data*. 2005. 16
- 695 [29] "Libpng open source reference library." <http://www.libpng.org/pub/png/libpng.html>. 28